

Particle, kinetic and hydrodynamic models for sea ice floes.

Part II: Rotating floes with nonlinear contact forces

Quanling Deng* Seung-Yeal Ha[†] Jaemoon Lee[‡]

Abstract

This paper extends the multiscale modeling framework introduced in Part I (Deng and Ha, *Physica D: Nonlinear Phenomena* 483 (2025) 134951) for sea-ice floe dynamics with non-rotating floes to the case with rotational floes and nonlinear contact interactions. Building on the particle–kinetic–hydrodynamic hierarchy developed for non-rotating floes, we generalize the particle model to describe ice floes as rigid bodies characterized by position, linear velocity, angular velocity, size, and moment of inertia. The interaction rules now include nonlinear contact forces and torques arising from short-range compression, restitution, and tangential friction laws, together with hydrodynamic drag that couples translational and rotational motions. These particle descriptions lead to an enriched Vlasov-type kinetic equation posed on an extended phase space, whose moments yield a hydrodynamic system for mass, momentum, and angular-momentum balances. Compared with Part I, the resulting macroscopic equations feature additional stress contributions, rotational transport, and dissipative mechanisms stemming from nonlinear collisions. The proposed framework provides a more realistic description of sea-ice floe dynamics and offers a systematic pathway toward multiscale modeling of sea-ice rheology under complex environmental forcing.

Keywords: Sea ice floe dynamics, Hertz contact mechanics, energy dissipation, mean-field approximation, hydrodynamic limit.

1 Introduction

Sea ice plays a fundamental role in Earth’s polar climate system by regulating heat exchange, momentum transfer, and biogeochemical processes at the ocean–atmosphere interface. Its dynamics emerge from the complex interplay between environmental forcing, including wind, ocean currents, and waves, and mechanical interactions among heterogeneous floes (c.f., [1, 2, 7, 27, 46, 55, 58, 61]). In the Marginal Ice Zone (MIZ), where

*Yau Mathematical Sciences Center, Tsinghua University, Beijing, 100084, China (qldeng@tsinghua.edu.cn); School of Computing, Australian National University, Canberra, ACT 2601, Australia (quanling.deng@anu.edu.au).

[†]Department of Mathematical Sciences and Research Institute of Mathematics, Seoul National University, Seoul 08826, Republic of Korea (syha@snu.ac.kr).

[‡]Department of Mathematical Sciences, Seoul National University, Seoul 08826, Republic of Korea (dlwoans0001@snu.ac.kr).

the ice cover is highly fragmented, individual floe-floe interactions dominate the mechanical behavior of the ice pack, often giving rise to phenomena that are more naturally described by particle floes (c.f., [5, 6]).

Continuum-based models, such as elastic-plastic [16], viscous-plastic [42, 63], elastic-viscous-plastic [45], and Maxwell-type rheological models [19], have been developed for simulating the large-scale behavior of compact ice packs (for ice sheets and glaciers, we refer to, e.g., [57]). However, the continuum assumption can break down in both large and small scales in the MIZ or other areas [68], where collisions, heterogeneity, and anisotropic deformation fields produce granular-like behavior that cannot be adequately represented by homogenized constitutive laws. These limitations have motivated the development of particle-based (discrete element) approaches [4, 18, 20, 43, 52, 54, 69], which explicitly represent sea ice as a collection of rigid bodies and naturally capture processes such as collisions, ridging, rafting, and fracture patterns. In earlier model developments, Gudkovich *et al.* [34] studied the dynamics of an individual floe in 1963, based on the observations of Nansen [56] in 1902, and developed a model to describe the speed and direction of drift depended on floe size and shape. Future directions for sea ice modelling are also discussed here [7, 29, 47].

A key challenge in particle-based modeling lies in accurately representing contact interactions. Nonlinear contact mechanics, including Hertzian-type normal forces, velocity-dependent restitution, tangential friction laws, and torque transfer at contact points, play a critical role in determining floe trajectories and rotational dynamics. Such nonlinear collision models, widely used in granular and rigid-body simulations [17, 48], have recently been applied to sea ice floes [38]. Rotational degrees of freedom further enrich the dynamics: collisions generate torques, frictional impulses modify angular momentum, and ocean drag acts simultaneously on translational and rotational motions. These effects contribute to complex behaviors such as spin alignment, rotational clustering, collision-induced jamming, and enhanced dissipation, all observed in high-resolution DEM studies [38].

In Part I of this series [23], we have developed a particle-kinetic-hydrodynamic hierarchy for non-rotating cylindrical floes governed by linear contact forces. That formulation established a systematic pathway from Newtonian-type particle models to Vlasov-type kinetic descriptions and further to hydrodynamic equations based on velocity moments. While the non-rotating framework provides conceptual clarity, it neglects nonlinear contact mechanics and rotational effects that are essential for accurately capturing sea-ice behavior in fragmented regimes.

The present paper extends the multiscale framework of Part I by incorporating rotational degrees of freedom and nonlinear contact forces into the particle, kinetic, and hydrodynamic descriptions. This provides a pathway to couple particle and continuum models within a multiscale framework [24], together with their integration into data assimilation schemes [14, 15, 21], enabling more accurate predictions. At the particle level, each floe is modeled as a rigid body characterized by its position, orientation, linear velocity, angular velocity, size, and moment of inertia. Collisions generate both forces and torques, described through physically realistic nonlinear force laws and frictional

interactions. This leads to a richer kinetic formulation defined on an extended phase space that includes angular velocities and orientations. Suitable moment closures then yield hydrodynamic equations that track mass, linear momentum, and angular momentum, together with stress and couple-stress contributions arising from torque-generating interactions. The objective of this Part II work is to establish a rigorous theoretical foundation for such a rotating particle–kinetic–hydrodynamic hierarchy. Our main contributions include:

- a rigorous study on the behavior of total momentum and energy of a particle model for rotating floes with nonlinear contact forces;
- the derivation of a kinetic model on an extended phase space incorporating rotational dynamics, followed by a study on the momentum and energy;
- the development and study of a hydrodynamic system that captures macroscopic evolution of both linear and angular momentum and energies.

The rest of the paper is organized as follows. In Section 2, we introduce the rotating sea-ice floe particle model with nonlinear contact laws in Subsection 2.1, followed by a study on the asymptotic behavior of total momentum and energy in Subsection 2.2. In Section 3 and Section 4, we present the corresponding kinetic description using the mean-field limit, followed by a hydrodynamic model with monokinetic closure. We also study the asymptotic behavior on momentum and energies of these models. In Section 5, we provide several numerical examples to validate our theoretical findings. Finally, Section 6 is devoted to the summary of the paper with a discussion of the main findings and future directions.

2 Particle description for ice floes

In this section, we introduce the particle model for the ice floes with rotation and nonlinear Hertzian contact forcing, followed by a study on its asymptotic collective behavior on momentum and energy.

2.1 The particle model

Consider colliding ice floes with the geometry of cylinders. Given a system of n floes, we denote by r^i the radius and h^i the thickness (or height) of the i -th floe with $i \in [n] := \{1, 2, \dots, n\}$. The radius and thickness characterize the floe size. In a realistic sea ice floe setting (particularly in marginal ice zones), the floe size often follow a power law distribution [64], while the floe thickness distribution follows a Gamma distribution (see, for example, [11, 65, 66] for the Arctic region and [67] for the Antarctic region). The mass of the i -th floe is $m^i = \rho_{ice}\pi(r^i)^2h^i$, where the constant ρ_{ice} is the density of sea ice floes. We assume that the mass of each floe does not change over time (thus, no melting, freezing, or fracturing). We denote by $I^i = m^i(r^i)^2$ the moment of inertia. The floe position is denoted by $\mathbf{x}^i = (x^i, y^i)^T$ and the floe velocity is $\mathbf{v}^i = (u^i, v^i)^T$. We denote

the floe angular location as θ^i and angular velocity as $\omega^i \hat{z}$. Herein, \hat{z} is the unit vector along the z -axis (perpendicular to the (x, y) plane). We consider the angular velocity as a scalar in this dimension and omit the multiplication of \hat{z} for simplicity. Thus, if the result of the cross product is a vector along the z -axis, we consider it as a z -value scalar as in (2.1b) and (2.1d) below. Lastly, let $\mathbf{u}_o = \mathbf{u}_o(x, y)$ be the given ocean surface velocity. The governing equations of rotating-colliding sea ice floe dynamics are given by Newton's equations:

$$\frac{d\mathbf{x}^i}{dt} = \mathbf{v}^i, \quad i \in [n], \quad (2.1a)$$

$$\frac{d\theta^i}{dt} = \omega^i, \quad (2.1b)$$

$$m^i \frac{d\mathbf{v}^i}{dt} = \frac{1}{n} \sum_{j=1}^n (\mathbf{f}_n^{ij} + \mathbf{f}_t^{ij}) + \alpha^i (\mathbf{u}_o^i - \mathbf{v}^i) |\mathbf{u}_o^i - \mathbf{v}^i| := \mathbf{F}^i, \quad (2.1c)$$

$$I^i \frac{d\omega^i}{dt} = \frac{1}{n} \sum_{j=1}^n (r^i \mathbf{n}^{ij} \times \mathbf{f}_t^{ij}) + \beta^i (\nabla \times \mathbf{u}_o^i / 2 - \omega^i) |\nabla \times \mathbf{u}_o^i / 2 - \omega^i| := T^i, \quad (2.1d)$$

where $|\cdot|$ is the ℓ^2 -norm and

$$\begin{aligned} \mathbf{f}_n^{ij} &= (\kappa_1^{ij} \delta^{ij} + \kappa_2^{ij} (\mathbf{v}^i - \mathbf{v}^j) \cdot \mathbf{n}^{ij}) \mathbf{n}^{ij}, \\ \mathbf{f}_t^{ij} &= \zeta^{ij} \tilde{\mathbf{f}}_t^{ij}, \quad \tilde{\mathbf{f}}_t^{ij} = \kappa_3^{ij} \sigma^{ij} \mathbf{t}^{ij}, \\ \kappa_1^{ij} &= \pi E_e \chi^{ij} h_e^{ij} g \left(\frac{\delta^{ij} r_e^{ij}}{2(h_e^{ij})^2} \right), \quad g(\xi) = \frac{0.9117\xi^2 - 0.2722\xi + 0.003324}{\xi^2 - 1.524\xi + 0.03159} \\ \kappa_2^{ij} &= \eta \sqrt{5\kappa_1^{ij} m_e^{ij}}, \quad \kappa_3^{ij} = 6 \frac{G_e}{E_e} \kappa_1^{ij}, \\ \delta^{ij} &= d^{ij} - (r^i + r^j), \quad \text{with } d^{ij} = |\mathbf{x}^i - \mathbf{x}^j|, \\ \sigma_t^{ij} &= \frac{d\sigma^{ij}}{dt} = (\mathbf{v}^j - \mathbf{v}^i) \cdot \mathbf{t}^{ij} - r^j \omega^j - r^i \omega^i, \\ \sigma^{ij} &= \int_{t_{\text{start}}}^t \sigma_t^{ij}(s) ds = t_c^{ij} \sigma_t^{ij}, \quad t_c^{ij} \approx 2.94 \left(\frac{m_e^{ij}}{\kappa_1^{ij}} \right)^{2/5} |v_i - v_j|^{-1/5}, \\ \alpha^i &= \pi \rho_o (2C_{v,o} r^i \cdot D^i + C_{h,o} (r^i)^2), \\ \beta^i &= \pi (r^i)^4 \rho_o (C_{v,o} D^i + r^i C_{h,o} / 5). \end{aligned} \quad (2.2)$$

We discuss the physical quantities and parameters one by one below. First,

$$E_e = \frac{E}{2(1-\nu^2)}, \quad G_e = \frac{E}{4(2+\nu)(1-\nu)}, \quad (2.3)$$

where E is Young's modulus, and ν is Poisson's ratio (assuming the same for all floes). In the integration for σ^{ij} , t_{start} specifies the starting time of the collision, and t_c^{ij} is

an approximate contact duration time that compensates the integration [35]. χ is a characteristic function

$$\chi^{ij} = \begin{cases} 1, & \text{when } i \neq j \text{ and } \delta^{ij} < 0, \\ 0, & \text{otherwise,} \end{cases} \quad (2.4)$$

which characterizes whether floes i and j are in contact or not. We multiply this by κ_1^{ij} for notational simplicity. \mathbf{f}_n^{ij} and \mathbf{f}_t^{ij} are normal and tangential components of the contact force, respectively. For notational convenience, we denote $\mathbf{f}_c^{ij} = \mathbf{f}_n^{ij} + \mathbf{f}_t^{ij}$ with the auxiliary parameter ζ defined as

$$\zeta^{ij} = \begin{cases} 1, & \text{when } |\tilde{\mathbf{f}}_t^{ij}| \leq \mu |\mathbf{f}_n^{ij}|, \\ \frac{\mu |\mathbf{f}_n^{ij}|}{|\tilde{\mathbf{f}}_t^{ij}|}, & \text{otherwise.} \end{cases} \quad (2.5)$$

This imposes the Coulomb friction law that plays an important role in limiting the tangential contact force relative to the magnitude of the normal contact force [43]:

$$|\mathbf{f}_t^{ij}| \leq \mu |\mathbf{f}_n^{ij}|,$$

where μ is the coefficient of friction that characterizes the condition of the surfaces of two floes in contact.

We assume zero tangential damping as in [17, 18]. The floe contact force \mathbf{F}^i and torque T^i are non-zero only when two floes are in contact, i.e., $\delta^{ij} < 0$. We also remark that for $\delta^{ij} < 0$, we have $\xi < 0$ and $g(\xi) > 0$. This guarantees the correct sign of $\kappa_1^{ij} \delta^{ij}$ in the term \mathbf{f}_n^{ij} . We follow the Hertz contact theory [41, 60] and adopt the model for the normal contact force (see the supplementary material of [38]). By default, $i \neq j$, $i, j \in [n]$. We assume $\delta^{ij} = 0$ when $i = j$ (hence, $\mathbf{f}_n^{ij} = \mathbf{f}_t^{ij} = \mathbf{0}$) for notational simplicity. σ_t^{ij} is the slip-rate along the tangential direction caused by both translation and rotation (relative contact velocity projected in the tangential direction). σ is the rotational deformation, i.e., the tangential shear deformation. ρ_o is ocean density, D^i is the ice-floe draft (the part of the ice floe below the water surface), $C_{v,o}$ is ocean vertical drag coefficients, $C_{h,o}$ is ocean horizontal drag coefficients. In default, we set $D^i = 0.9h^i$.

The vector $\mathbf{n}^{ij} := \frac{\mathbf{x}^j - \mathbf{x}^i}{|\mathbf{x}^j - \mathbf{x}^i|}$ is the unit normal vector pointing from the center of floe i to floe j (if $i = j$, let it be \mathbf{z}), \mathbf{t}^{ij} is the unit vector along the tangential direction (rotating \mathbf{n}^{ij} counterclockwise by 90°), \mathbf{r}^j is the radius multiplied by the associated normal vector pointing towards the center of the j -th floe, E_e is the effective contact modulus, $h_e^{ij} := \min\{h^i, h^j\}$ is the effective contact thickness (part of the thickness in contact), $m_e^{ij} := \frac{m^i m^j}{m^i + m^j}$ is the effective mass, $r_e^{ij} := \frac{r^i r^j}{r^i + r^j}$ is the effective radius, and

$$\eta := \frac{\ln e_r}{\sqrt{\ln^2 e_r + \pi^2}} < 0. \quad (2.6)$$

Here e_r is the restitution coefficient in $[0, 1)$. The restitution coefficient for ice floes is a measure of kinetic energy loss during floe collisions. The coefficient is usually a positive

real number between 0 and 1. A value of 0 indicates a perfectly inelastic collision, while a value of 1 indicates a perfectly elastic collision. The typical values of e_r for sea ice are between 0.1 and 0.3; see [51]. In ice floe studies, values between 0 and 1 are often employed; see, for example [40]. Details are referred to equations (1), (8), (20), and (26) in the supplementary material of [38]. We scale the summation of the contact force by the factor of $1/n$ to apply the mean-field theory for deriving the kinetic and hydrodynamic models. For a system with a fixed number of floes, this scaling factor may be understood as a factor of the mass and drag coefficient.

2.2 Asymptotic behavior

To study the asymptotic behavior of the particle model (2.1), we first define the strain and kinetic energies. The normal strain energy for two colliding floes is defined as

$$M_{2,\mathbf{x}}^{ij} := \int_0^{\delta^{ij}} \mathbf{f}_{\mathbf{n},s}^{ij} ds = \int_0^{\delta^{ij}} \kappa_1^{ij}(s) ds.$$

This normal strain energy evolves with respect to time. Using the Leibniz integral rule, we have

$$\frac{dM_{2,\mathbf{x}}^{ij}}{dt} = \frac{d}{dt} \int_0^{\delta^{ij}} \kappa_1^{ij}(s) ds = \kappa_1^{ij}(\delta^{ij}) \delta^{ij} \frac{d\delta^{ij}}{dt}. \quad (2.7)$$

With this in mind, we define the floe moments as follows:

$$\begin{aligned} M_0 &= \sum_{i=1}^n m^i, & \mathbf{M}_{1,\mathbf{v}} &= \sum_{i=1}^n m^i \mathbf{v}^i, & M_{1,\omega} &= \sum_{i=1}^n (m^i \mathbf{x}^i \times \mathbf{v}^i + I^i \omega^i), \\ M_2 &= M_{2,\mathbf{v}} + M_{2,\mathbf{x}} + M_{2,\omega}, \\ M_{2,\mathbf{v}} &= \frac{1}{2} \sum_{i=1}^n m^i |\mathbf{v}^i|^2, & M_{2,\mathbf{x}} &= \frac{1}{2n} \sum_{i,j=1}^n M_{2,\mathbf{x}}^{ij}, & M_{2,\omega} &= \frac{1}{2} \sum_{i=1}^n I^i (\omega^i)^2, \end{aligned} \quad (2.8)$$

where M_0 is the zero-order moment, i.e., total mass. $\mathbf{M}_{1,\mathbf{v}}$ is the total momentum. $M_{1,\omega}$ is the total angular momentum, which includes the orbital angular momentum (due to translational motion) and the spin angular momentum (due to rotation about the center of mass). $M_{2,\mathbf{x}}$, $M_{2,\mathbf{v}}$, $M_{2,\omega}$, and M_2 represent the total normal strain energy, the total translational kinetic energy, the total rotational kinetic energy, and the total energy, respectively. The scaling $\frac{1}{n}$ in $M_{2,\mathbf{x}}$ ensures that total strain energy remain $\mathcal{O}(1)$ in the mean-field limit as $n \rightarrow \infty$. Note that each energies are by definition positive.

Lemma 2.1 (Total momentum balances). *Let $(\mathbf{x}^i, \mathbf{v}^i, \theta^i, \omega^i)$ be a global solution to the system (2.1). Then, the following assertions hold.*

1. *The total linear momentum satisfies*

$$\frac{d\mathbf{M}_{1,\mathbf{v}}}{dt} = \sum_{i=1}^n \alpha^i (\mathbf{u}_o^i - \mathbf{v}^i) |\mathbf{u}_o^i - \mathbf{v}^i|. \quad (2.9)$$

2. The total angular momentum satisfies

$$\frac{dM_{1,\omega}}{dt} = \sum_{i=1}^n [\alpha^i \mathbf{x}^i \times (\mathbf{u}_o^i - \mathbf{v}^i) |\mathbf{u}_o^i - \mathbf{v}^i| + \beta^i (\nabla \times \mathbf{u}_o^i/2 - \omega^i) |\nabla \times \mathbf{u}_o^i/2 - \omega^i|]. \quad (2.10)$$

Proof. For the first assertion, we first note that the relations

$$\delta^{ij} = \delta^{ji}, \quad \mathbf{n}^{ij} = -\mathbf{n}^{ji}, \quad \mathbf{t}^{ij} = -\mathbf{t}^{ji}, \quad i, j \in [n],$$

to see the anti-symmetry of the floe-floe contact force:

$$\mathbf{f}_n^{ij} = -\mathbf{f}_n^{ji}, \quad \mathbf{f}_t^{ij} = -\mathbf{f}_t^{ji}, \quad i, j \in [n]. \quad (2.11)$$

Now, we use (2.1), (2.8), and (2.11) to find

$$\begin{aligned} \frac{dM_{1,v}}{dt} &= \frac{d}{dt} \sum_{i=1}^n m^i \mathbf{v}^i = \sum_{i=1}^n m^i \frac{d\mathbf{v}^i}{dt} = \sum_{i=1}^n \left(\frac{1}{n} \sum_{j=1}^n (\mathbf{f}_n^{ij} + \mathbf{f}_t^{ij}) + \alpha^i (\mathbf{u}_o^i - \mathbf{v}^i) |\mathbf{u}_o^i - \mathbf{v}^i| \right) \\ &= \frac{1}{n} \sum_{i,j=1}^n (\mathbf{f}_n^{ij} + \mathbf{f}_t^{ij}) + \sum_{i=1}^n \alpha^i (\mathbf{u}_o^i - \mathbf{v}^i) |\mathbf{u}_o^i - \mathbf{v}^i| = \sum_{i=1}^n \alpha^i (\mathbf{u}_o^i - \mathbf{v}^i) |\mathbf{u}_o^i - \mathbf{v}^i|. \end{aligned}$$

For the second claim, using (2.1) and the property of the cross product $\mathbf{v}^i \times \mathbf{v}^i = 0$, we calculate

$$\begin{aligned} \frac{dM_{1,\omega}}{dt} &= \frac{d}{dt} \sum_{i=1}^n (m^i \mathbf{x}^i \times \mathbf{v}^i + I^i \omega^i) \\ &= \sum_{i=1}^n \left(m^i \frac{d\mathbf{x}^i}{dt} \times \mathbf{v}^i + m^i \mathbf{x}^i \times \frac{d\mathbf{v}^i}{dt} + I^i \frac{d\omega^i}{dt} \right) \\ &= \sum_{i=1}^n \left(\mathbf{x}^i \times m^i \frac{d\mathbf{v}^i}{dt} + I^i \frac{d\omega^i}{dt} \right) \\ &= \sum_{i=1}^n \left(\mathbf{x}^i \times \left(\frac{1}{n} \sum_{j=1}^n (\mathbf{f}_n^{ij} + \mathbf{f}_t^{ij}) + \alpha^i (\mathbf{u}_o^i - \mathbf{v}^i) |\mathbf{u}_o^i - \mathbf{v}^i| \right) \right. \\ &\quad \left. + \left(\frac{1}{n} \sum_{j=1}^n (r^i \mathbf{n}^{ij} \times \mathbf{f}_t^{ij}) + \beta^i (\nabla \times \mathbf{u}_o^i/2 - \omega^i) |\nabla \times \mathbf{u}_o^i/2 - \omega^i| \right) \right) \\ &=: \mathcal{T}_a + \mathcal{T}_b, \end{aligned}$$

where

$$\begin{aligned} \mathcal{T}_a &= \frac{1}{n} \sum_{i,j=1}^n (\mathbf{x}^i \times (\mathbf{f}_n^{ij} + \mathbf{f}_t^{ij}) + (r^i \mathbf{n}^{ij} \times \mathbf{f}_t^{ij})), \\ \mathcal{T}_b &= \sum_{i=1}^n (\alpha^i \mathbf{x}^i \times (\mathbf{u}_o^i - \mathbf{v}^i) |\mathbf{u}_o^i - \mathbf{v}^i| + \beta^i (\nabla \times \mathbf{u}_o^i/2 - \omega^i) |\nabla \times \mathbf{u}_o^i/2 - \omega^i|). \end{aligned}$$

We denote the contact point of floes i and j as \mathbf{c}^{ij} . Then we have

$$\mathbf{c}^{ij} = \mathbf{x}^i + r^i \mathbf{n}^{ij}, \quad \mathbf{c}^{ji} = \mathbf{x}^j + r^j \mathbf{n}^{ji}, \quad \mathbf{c}^{ij} = \mathbf{c}^{ji}. \quad (2.12)$$

Using (2.12), anti-symmetry, and $(\mathbf{x}^i - \mathbf{x}^j) \times \mathbf{n}^{ij} = 0$, we calculate

$$\begin{aligned} \mathcal{T}_a &= \frac{1}{n} \sum_{i,j=1}^n \mathbf{x}^i \times \mathbf{f}_n^{ij} + \frac{1}{n} \sum_{i,j=1}^n (\mathbf{x}^i \times \mathbf{f}_t^{ij} + (r^i \mathbf{n}^{ij} \times \mathbf{f}_t^{ij})) \\ &= -\frac{1}{n} \sum_{i,j=1}^n \mathbf{x}^j \times \mathbf{f}_n^{ij} + \frac{1}{n} \sum_{i,j=1}^n \mathbf{c}^{ij} \times \mathbf{f}_t^{ij} \\ &= \frac{1}{2n} \sum_{i,j=1}^n (\mathbf{x}^i - \mathbf{x}^j) \times \mathbf{f}_n^{ij} + \frac{1}{2n} \sum_{i,j=1}^n (\mathbf{c}^{ij} \times \mathbf{f}_t^{ij} + \mathbf{c}^{ji} \times \mathbf{f}_t^{ji}) \\ &= 0. \end{aligned} \quad (2.13)$$

This leads to the desired result for the balance law of total angular momentum. \square

Remark 2.2. In the derivation of (2.13), we used the contact point assumption/equality (2.12), which implies $\delta^{ij} = 0$. This distinguishes it from the contact deformation assumption for computing the normal contact force. That is, we assume that the floe particles deform upon contact, and the overlap (deformation) δ^{ij} is used to compute the contact forces \mathbf{f}_n^{ij} and \mathbf{f}_t^{ij} . However, when computing torques, we assume that the contact occurs at a point located *on the undeformed geometry*, i.e., at a distance $r^i \mathbf{n}^{ij}$ from the center. This introduces a modeling approximation, which is justified in [53, 59]:

1. **Deformations are small:** In most sea ice floe particle settings, overlaps are very small compared to particle size, so undeformed geometry introduces only second-order errors.
2. **Approximate consistency:** The total torque from each force pair cancels under Newton's third law, ensuring conservation of angular momentum.

Lemma 2.3 (Total energy balance). *Let $(\mathbf{x}^i, \mathbf{v}^i, \theta^i, \omega^i)$ be a global solution to system (2.1). Then, the following relation holds:*

$$\begin{aligned} \frac{dM_2}{dt} &= \frac{1}{2n} \sum_{i,j=1}^n \kappa_2^{ij} |(\mathbf{v}^i - \mathbf{v}^j) \cdot \mathbf{n}^{ij}|^2 - \frac{1}{2n} \sum_{i,j=1}^n \zeta^{ij} \kappa_3^{ij} t_c^{ij} (\sigma_t^{ij})^2 \\ &\quad + \sum_{i=1}^n \alpha^i (\mathbf{u}_o^i - \mathbf{v}^i) |\mathbf{u}_o^i - \mathbf{v}^i| \cdot \mathbf{v}^i \\ &\quad + \sum_{i=1}^n \beta^i \omega^i (\nabla \times \mathbf{u}_o^i / 2 - \omega^i) |\nabla \times \mathbf{u}_o^i / 2 - \omega^i|. \end{aligned} \quad (2.14)$$

Proof. We take the product of (2.1c) with \mathbf{v}^i , and sum up the resulting equations over all $i \in [n]$ to obtain

$$\begin{aligned}
\frac{dM_{2,\mathbf{v}}}{dt} &= \sum_{i=1}^n m^i \frac{d\mathbf{v}^i}{dt} \cdot \mathbf{v}^i = \sum_{i=1}^n \left(\frac{1}{n} \sum_{j=1}^n (\mathbf{f}_n^{ij} + \mathbf{f}_t^{ij}) + \alpha^i (\mathbf{u}_o^i - \mathbf{v}^i) |\mathbf{u}_o^i - \mathbf{v}^i| \right) \cdot \mathbf{v}^i \\
&= \frac{1}{n} \sum_{i,j=1}^n (\kappa_1^{ij} \delta^{ij} + \kappa_2^{ij} (\mathbf{v}^i - \mathbf{v}^j) \cdot \mathbf{n}^{ij}) \mathbf{n}^{ij} \cdot \mathbf{v}^i + \frac{1}{n} \sum_{i,j=1}^n \mathbf{f}_t^{ij} \cdot \mathbf{v}^i \\
&\quad + \sum_{i=1}^n \alpha^i (\mathbf{u}_o^i - \mathbf{v}^i) |\mathbf{u}_o^i - \mathbf{v}^i| \cdot \mathbf{v}^i \\
&=: \mathcal{T}_{11} + \mathcal{T}_{12} + \mathcal{T}_{13} + \sum_{i=1}^n \alpha^i (\mathbf{u}_o^i - \mathbf{v}^i) |\mathbf{u}_o^i - \mathbf{v}^i| \cdot \mathbf{v}^i.
\end{aligned} \tag{2.15}$$

Below, we estimate the terms \mathcal{T}_{1i} , $i = 1, 2$, one by one. For \mathcal{T}_{13} , we estimate it combined with the angular velocity component afterwards.

- Case A.1: We use (2.1a) and the relations:

$$\delta^{ij} = \delta^{ji}, \quad \mathbf{n}^{ij} = -\mathbf{n}^{ji}$$

to rewrite

$$\begin{aligned}
\mathcal{T}_{11} &= \frac{1}{n} \sum_{i,j=1}^n \kappa_1^{ij} \delta^{ij} \mathbf{n}^{ij} \cdot \frac{d\mathbf{x}^i}{dt} = -\frac{1}{n} \sum_{i,j=1}^n \kappa_1^{ij} \delta^{ij} \mathbf{n}^{ij} \cdot \frac{d\mathbf{x}^j}{dt} \\
&= -\frac{1}{2n} \sum_{i,j=1}^n \kappa_1^{ij} \delta^{ij} \mathbf{n}^{ij} \cdot \frac{d(\mathbf{x}^j - \mathbf{x}^i)}{dt} \\
&= -\frac{1}{2n} \sum_{i,j=1}^n \kappa_1^{ij} \delta^{ij} \cdot \frac{d\delta^{ij}}{dt} = -\frac{dM_{2,\mathbf{x}}}{dt},
\end{aligned} \tag{2.16}$$

where we used (2.7) and the following identity:

$$\begin{aligned}
\frac{d\delta^{ij}}{dt} &= \frac{d}{dt} (|\mathbf{x}^i - \mathbf{x}^j| - (r^i + r^j)) = \frac{d}{dt} \sqrt{(x^j - x^i)^2 + (y^j - y^i)^2} \\
&= \frac{2(x^j - x^i)d(x^j - x^i) + 2(y^j - y^i)d(y^j - y^i)}{2\sqrt{(x^j - x^i)^2 + (y^j - y^i)^2}dt} = \mathbf{n}^{ij} \cdot \frac{d(\mathbf{x}^j - \mathbf{x}^i)}{dt}.
\end{aligned}$$

- Case A.2: Similarly, we have

$$\begin{aligned}
\mathcal{T}_{12} &= \frac{1}{n} \sum_{i,j=1}^n \kappa_2^{ij} ((\mathbf{v}^i - \mathbf{v}^j) \cdot \mathbf{n}^{ij}) \mathbf{n}^{ij} \cdot \mathbf{v}^i = -\frac{1}{n} \sum_{i,j=1}^n \kappa_2^{ij} ((\mathbf{v}^i - \mathbf{v}^j) \cdot \mathbf{n}^{ij}) \mathbf{n}^{ij} \cdot \mathbf{v}^j \\
&= \frac{1}{2n} \sum_{i,j=1}^n \kappa_2^{ij} ((\mathbf{v}^i - \mathbf{v}^j) \cdot \mathbf{n}^{ij})^2.
\end{aligned} \tag{2.17}$$

For rotational kinetic energy, we take an inner product of (2.1d) with ω^i , and sum up the resulting equations over all $i \in [n]$ to get

$$\begin{aligned}
\frac{dM_{2,\omega}}{dt} &= \sum_{i=1}^n I^i \frac{d\omega^i}{dt} \cdot \omega^i \\
&= \sum_{i=1}^n \left(\frac{1}{n} \sum_{j=1}^n (r^i \mathbf{n}^{ij} \times \mathbf{f}_t^{ij}) + \beta^i (\nabla \times \mathbf{u}_o^i/2 - \omega^i) |\nabla \times \mathbf{u}_o^i/2 - \omega^i| \right) \cdot \omega^i \\
&= \frac{1}{n} \sum_{i,j=1}^n r^i \mathbf{n}^{ij} \times \mathbf{f}_t^{ij} \omega^i + \sum_{i=1}^n \beta^i \omega^i (\nabla \times \mathbf{u}_o^i/2 - \omega^i) |\nabla \times \mathbf{u}_o^i/2 - \omega^i| \\
&=: \mathcal{T}_{14} + \sum_{i=1}^n \beta^i \omega^i (\nabla \times \mathbf{u}_o^i/2 - \omega^i) |\nabla \times \mathbf{u}_o^i/2 - \omega^i|.
\end{aligned} \tag{2.18}$$

Using the definition (2.2) and the facts that $\mathbf{n}^{ij} \times \mathbf{t}^{ij} = 1$ and $\mathbf{t}^{ij} \cdot \mathbf{t}^{ij} = 1$, we now calculate $\mathcal{T}_{1,3} + \mathcal{T}_{1,4}$ below:

$$\begin{aligned}
\mathcal{T}_{1,3} + \mathcal{T}_{1,4} &= \frac{1}{n} \sum_{i,j=1}^n \mathbf{f}_t^{ij} \cdot \mathbf{v}^i + \frac{1}{n} \sum_{i,j=1}^n \mathbf{n}^{ij} \times \mathbf{f}_t^{ij} r^i \omega^i \\
&= -\frac{1}{n} \sum_{i,j=1}^n \mathbf{f}_t^{ij} \cdot \mathbf{v}^j + \frac{1}{n} \sum_{i,j=1}^n \mathbf{n}^{ij} \times \mathbf{f}_t^{ij} r^j \omega^j \\
&= \frac{1}{2n} \sum_{i,j=1}^n \mathbf{f}_t^{ij} \cdot (\mathbf{v}^i - \mathbf{v}^j) + \frac{1}{2n} \sum_{i,j=1}^n \mathbf{n}^{ij} \times \mathbf{f}_t^{ij} (r^i \omega^i + r^j \omega^j) \\
&= \frac{1}{2n} \sum_{i,j=1}^n \mathbf{f}_t^{ij} \cdot [(\mathbf{v}^i - \mathbf{v}^j) \cdot \mathbf{t}^{ij}] \mathbf{t}^{ij} + \frac{1}{2n} \sum_{i,j=1}^n \mathbf{f}_t^{ij} \cdot (r^i \omega^i + r^j \omega^j) \mathbf{t}^{ij} \\
&= -\frac{1}{2n} \sum_{i,j=1}^n \mathbf{f}_t^{ij} \cdot \sigma_t^{ij} \mathbf{t}^{ij} \\
&= -\frac{1}{2n} \sum_{i,j=1}^n \zeta^{ij} \kappa_3^{ij} t_c^{ij} (\sigma_t^{ij})^2.
\end{aligned} \tag{2.19}$$

Summing up the above estimates in (2.15) with terms (2.16), (2.17), and (2.18) with term (2.19) gives the desired estimate for the total energy. \square

Lemma 2.4 (Total energy lower bound). *Let $(\mathbf{x}^i, \mathbf{v}^i, \theta^i, \omega^i)$ be a global solution to the system (2.1). Assume a uniform bound on the duration of contact time, i.e., $t_c^{ij} < t_c^{\max}$. If $\alpha^i = \beta^i = 0, \forall i \in [n]$, then there exist positive constants A_0 and A_1 such that*

$$M_2(t) \geq M_2(0)e^{-A_0 t} + \frac{A_1}{A_0} |\mathbf{M}_{1,\mathbf{v}}(0)|^2 (1 - e^{-A_0 t}).$$

Proof. With

$$\alpha^i = \beta^i = 0, \quad \forall i \in [n],$$

the equalities (2.9) and (2.10) reduce to

$$\frac{dM_{1,\mathbf{v}}}{dt} = \mathbf{0}, \quad \frac{dM_{1,\omega}}{dt} = 0 \quad (2.20)$$

while the relation (2.14) reduces to

$$\frac{dM_2}{dt} = \frac{1}{2n} \sum_{i,j=1}^n \kappa_2^{ij} |(\mathbf{v}^i - \mathbf{v}^j) \cdot \mathbf{n}^{ij}|^2 - \frac{1}{2n} \sum_{i,j=1}^n \zeta^{ij} \kappa_3^{ij} t_c^{ij} (\sigma_t^{ij})^2.$$

Using the definition (2.2), the fact $\kappa_2^{ij} < 0$ (since $\eta < 0$ as in (2.6)), and the positivity of the other parameters, we observe

$$\frac{dM_2}{dt} \leq 0, \quad \text{i.e., total energy is dissipative.}$$

Now, we use the Cauchy–Schwarz inequality and boundedness of the mass of floe particles to see that there exist positive constants as the floe particle radii, thickness, and masses are fixed for a fixed system with n floes such that

$$\begin{aligned} & \frac{1}{2n} \sum_{i,j=1}^n |\kappa_2^{ij}| ((\mathbf{v}^j - \mathbf{v}^i) \cdot \mathbf{n}^{ij})^2 \\ & \leq \frac{1}{2n} \kappa_2^{\max} \sum_{i,j=1}^n |\mathbf{v}^j - \mathbf{v}^i|^2 \\ & \leq \frac{\kappa_2^{\max}}{2nm_{\min}^2} \sum_{i,j=1}^n m^i m^j |\mathbf{v}^j - \mathbf{v}^i|^2 \\ & = \frac{\kappa_2^{\max}}{2nm_{\min}^2} \sum_{i,j=1}^n m^i m^j (|\mathbf{v}^j|^2 + |\mathbf{v}^i|^2 - 2\mathbf{v}^i \cdot \mathbf{v}^j) \\ & \leq \frac{\kappa_2^{\max}}{2nm_{\min}^2} \left(2nm_{\max} \sum_{i=1}^n m^i |\mathbf{v}^i|^2 - 2 \left| \sum_{i=1}^n m^i \mathbf{v}^i \right|^2 \right) \\ & = \frac{\kappa_2^{\max} m_{\max}}{m_{\min}^2} \sum_{i=1}^n m^i |\mathbf{v}^i|^2 - \frac{\kappa_2^{\max}}{nm_{\min}^2} \left| \sum_{i=1}^n m^i \mathbf{v}^i \right|^2 \\ & := \mathcal{T}_{21} - \mathcal{T}_{22}, \end{aligned} \quad (2.21)$$

where $\kappa_2^{\max} = \max_{i,j} |\kappa_2^{ij}|$ and $m_{\min} = \min_i m^i$, $m_{\max} = \max_i m^i$.

By definition, we bound \mathcal{T}_{21}

$$\mathcal{T}_{21} = \frac{2\kappa_2^{\max} m_{\max}}{m_{\min}^2} M_{2,\mathbf{v}} \leq \frac{2\kappa_2^{\max} m_{\max}}{m_{\min}^2} M_2. \quad (2.22)$$

We use (2.20) to see

$$\mathcal{T}_{22} = \frac{\kappa_2^{\max}}{nm_{\min}^2} |\mathbf{M}_{1,\mathbf{v}}(0)|^2. \quad (2.23)$$

To bound the term $\frac{1}{2n} \sum_{i,j=1}^n \zeta^{ij} \kappa_3^{ij} t_c^{ij} (\sigma_t^{ij})^2$, we recall

$$\sigma_t^{ij} = (\mathbf{v}^j - \mathbf{v}^i) \cdot \mathbf{t}^{ij} - r^j \omega^j - r^i \omega^i, \quad |\mathbf{t}^{ij}| = 1.$$

Using $(a + b + c)^2 \leq 3(a^2 + b^2 + c^2)$ and $|(\mathbf{v}^j - \mathbf{v}^i) \cdot \mathbf{t}^{ij}| \leq |\mathbf{v}^j - \mathbf{v}^i|$,

$$(\sigma_t^{ij})^2 \leq 3 \left(|\mathbf{v}^j - \mathbf{v}^i|^2 + (r^j \omega^j)^2 + (r^i \omega^i)^2 \right).$$

With $\kappa_3^{ij} \leq \kappa_3^{\max} := \max_{i,j} \kappa_3^{ij}$ and $0 \leq \zeta^{ij} \leq 1$ by (2.5), we then have

$$\begin{aligned} \sum_{i,j=1}^n \zeta^{ij} \kappa_3^{ij} t_c^{ij} (\sigma_t^{ij})^2 &\leq \kappa_3^{\max} t_c^{\max} \sum_{i,j=1}^n (\sigma_t^{ij})^2 \\ &\leq 3\kappa_3^{\max} t_c^{\max} \sum_{i,j=1}^n \left(|\mathbf{v}^j - \mathbf{v}^i|^2 + (r^j \omega^j)^2 + (r^i \omega^i)^2 \right). \end{aligned} \quad (2.24)$$

We use

$$\sum_{i,j=1}^n |\mathbf{v}^j - \mathbf{v}^i|^2 = 2n \sum_{i=1}^n |\mathbf{v}^i|^2 - 2 \left| \sum_{i=1}^n \mathbf{v}^i \right|^2 \leq 2n \sum_{i=1}^n |\mathbf{v}^i|^2,$$

and

$$\sum_{i,j=1}^n \left((r^j \omega^j)^2 + (r^i \omega^i)^2 \right) = 2n \sum_{i=1}^n (r^i \omega^i)^2.$$

We substitute into (2.24) to find

$$\sum_{i,j=1}^n \zeta^{ij} \kappa_3^{ij} t_c^{ij} (\sigma_t^{ij})^2 \leq 6n\kappa_3^{\max} t_c^{\max} \left(\sum_{i=1}^n |\mathbf{v}^i|^2 + \sum_{i=1}^n (r^i \omega^i)^2 \right). \quad (2.25)$$

Similarly, we have

$$M_{2,\mathbf{v}} = \frac{1}{2} \sum_{i=1}^n m^i |\mathbf{v}^i|^2 \geq \frac{m_{\min}}{2} \sum_{i=1}^n |\mathbf{v}^i|^2 \quad \Rightarrow \quad \sum_{i=1}^n |\mathbf{v}^i|^2 \leq \frac{2}{m_{\min}} M_{2,\mathbf{v}}.$$

Moreover $I^i = m^i (r^i)^2 \geq m_{\min} (r^i)^2$, hence we have

$$I^i (\omega^i)^2 \geq m_{\min} (r^i \omega^i)^2 \quad \Rightarrow \quad \sum_{i=1}^n (r^i \omega^i)^2 \leq \frac{1}{m_{\min}} \sum_{i=1}^n I^i (\omega^i)^2 = \frac{2}{m_{\min}} M_{2,\omega}.$$

We put these into (2.25) to get

$$\frac{1}{2n} \sum_{i,j=1}^n \zeta^{ij} \kappa_3^{ij} t_c^{ij} (\sigma_t^{ij})^2 \leq \frac{6\kappa_3^{\max} t_c^{\max}}{m_{\min}} \left(M_{2,\mathbf{v}} + M_{2,\omega} \right) \leq \frac{6\kappa_3^{\max} t_c^{\max}}{m_{\min}} M_2.$$

Finally, we combine (2.24) with (2.21), (2.22) and (2.23) to obtain

$$\begin{aligned}\frac{dM_2}{dt} &\geq -\left(\frac{2\kappa_2^{\max}m_{\max}}{m_{\min}^2} + \frac{6\kappa_3^{\max}t_c^{\max}}{m_{\min}}\right)M_2 + \frac{\kappa_2^{\max}}{nm_{\min}^2}|\mathbf{M}_{1,\mathbf{v}}(0)|^2 \\ &=: -A_0M_2 + A_1|\mathbf{M}_{1,\mathbf{v}}(0)|^2.\end{aligned}$$

We use Grönwall's lemma [26, 33] to find the desired estimate. \square

Remark 2.5. Similar to the result [36] for the Cucker-Smale model, if the drag force is absent (i.e., $\alpha^i = \beta^i = 0$), Lemma 2.3 and Lemma 2.4 imply that the total energy M_2 is monotonically decreasing with a lower bound. Lemma 2.4 uses an assumption on the duration of contact t_c^{ij} . This is due to that the unregularized formula $t_c^{ij} \sim |\mathbf{v}^i - \mathbf{v}^j|^{-1/5}$ in (2.2) is not uniformly bounded as $|\mathbf{v}^i - \mathbf{v}^j| \rightarrow 0$. To obtain an energy-type estimate bound, one needs to remove this singularity. The common floe modeling practice [18, 38]: either (i) caps t_c^{ij} by a prescribed maximal contact time (often tied to time-step size dt in numerical simulation); or (ii) regularizes with a small $v_* > 0$ as

$$t_c^{ij} := 2.94\left(\frac{m_e^{ij}}{\kappa_1^{ij}}\right)^{2/5}\left(|\mathbf{v}^i - \mathbf{v}^j| + v_*\right)^{-1/5}, \quad v_* > 0.$$

On the other hand, Coulomb friction law imposed through ζ^{ij} also keeps the term $\sum_{i,j=1}^n \zeta^{ij} \kappa_3^{ij} t_c^{ij} (\sigma_t^{ij})^2$ from unbounded.

We now consider a special case where the ocean velocity is constant. In such a case, we show that the particle translational and rotational velocities are converging to constants. To establish this result rigorously, we first recall Barbalat's lemma to be used in later sections. It claims that if a uniformly continuous function is (Riemann)-integrable on the positive real line, then it converges to 0, as t goes to infinity.

Lemma 2.6 (Barbalat's Lemma). *Suppose that $f : \mathbb{R}_+ \rightarrow \mathbb{R}$ is a uniformly continuous function. If*

$$\int_0^\infty f(t)dt < \infty, \quad \implies \quad \lim_{t \rightarrow \infty} f(t) = 0.$$

Theorem 2.7. *Suppose that the given ocean surface velocity is constant:*

$$\mathbf{u}_o^i = \mathbf{u}_o^\infty : \text{constant}, \quad \forall i \in [n],$$

and let $(\mathbf{x}^i, \mathbf{v}^i, \theta^i, \omega^i)$ be a global solution to system (2.1). If $\alpha^i, \beta^i > 0$, we have

$$\lim_{t \rightarrow \infty} \|\mathbf{v}^i - \mathbf{u}_o^\infty\| = \mathbf{0}, \quad \lim_{t \rightarrow \infty} \omega^i(t) = 0, \quad \forall i \in [n].$$

Proof. Due to the translational invariance of system (2.1), we may assume that

$$\mathbf{u}_o^\infty \equiv \mathbf{0}$$

and we claim that

$$\lim_{t \rightarrow \infty} \mathbf{v}^i(t) = \mathbf{0}, \quad \lim_{t \rightarrow \infty} \omega^i(t) = 0. \quad (2.26)$$

It follows from Lemma 2.3 that

$$\frac{dM_2}{dt} \leq - \sum_{i=1}^n (\alpha^i |\mathbf{v}^i|^3 + \beta^i |\omega^i|^3), \quad (2.27)$$

where the first two terms in the right-hand side of (2.14) are negative (since $\kappa_2^{ij} < 0, \zeta \kappa_3^{ij} > 0$). Thus, total energy is non-increasing, which leads to boundedness of $\kappa_1^{ij} \delta^{ij}$, \mathbf{v}^i , and ω^i since each energy $M_{2,\mathbf{x}}$, $M_{2,\mathbf{v}}$, $M_{2,\omega}$ becomes bounded. Next, we integrate inequality (2.27),

$$\int_0^\infty \sum_{i=1}^n (\alpha^i |\mathbf{v}^i|^3 + \beta^i |\omega^i|^3) dt \leq M_2(0) - \inf_{t>0} M_2(t) \leq M_2(0),$$

to see that total energy is non-negative. Therefore, if we show that \mathbf{v}^i and ω^i are uniformly continuous, we can show that it tends to 0, by Barbalat's Lemma 2.6. We will prove it using the boundedness of $\dot{\mathbf{v}}^i$ and $\dot{\omega}^i$ (since the time derivative of the integrand of the above integral is these terms multiplied by bounded terms). Recall

$$\begin{aligned} m^i \frac{d\mathbf{v}^i}{dt} &= \frac{1}{n} \sum_{j=1}^n (\mathbf{f}_n^{ij} + \mathbf{f}_t^{ij}) - \alpha^i \mathbf{v}^i |\mathbf{v}^i|, \\ I^i \frac{d\omega^i}{dt} &= \frac{1}{n} \sum_{j=1}^n (r^i \mathbf{n}^{ij} \times \mathbf{f}_t^{ij}) - \beta^i \omega^i |\omega^i|, \end{aligned}$$

Under the boundedness of δ^{ij} , one can easily show the boundedness of κ_i coefficient terms and σ^{ij} , which leads to the boundedness of right-hand-side of the above equations. Therefore, \mathbf{v}^i and ω^i are uniformly continuous, which shows (2.26). \square

3 From particle to kinetic description

In this section, we first recall the formal derivation from the particle model to the kinetic model as the mean-field approximation of the particle model with $n \gg 1$. We assume that the number of particles involved in the particle system (2.1) is sufficiently large so that it becomes meaningful to use the mean-field approximation via the one-particle distribution function to describe the overall effective dynamics of the original system.

3.1 Kinetic model for ice floe dynamics

We first rewrite the floe particle model (2.1) as

$$\begin{cases} \frac{d\mathbf{x}^i}{dt} = \mathbf{v}^i, & \frac{d\theta^i}{dt} = \omega^i, & i \in [n], \\ \frac{d\mathbf{v}^i}{dt} = \frac{1}{m^i} \left[\frac{1}{n} \sum_{j=1}^n (\mathbf{f}_n^{ij} + \mathbf{f}_t^{ij}) + \alpha^i (\mathbf{u}_o^i - \mathbf{v}^i) |\mathbf{u}_o^i - \mathbf{v}^i| \right] =: \frac{\mathbf{F}^i}{m^i}, \\ \frac{d\omega^i}{dt} = \frac{1}{I^i} \left[\frac{1}{n} \sum_{j=1}^n (r^i \mathbf{n}^{ij} \times \mathbf{f}_t^{ij}) + \beta^i (\nabla \times \mathbf{u}_o^i / 2 - \omega^i) |\nabla \times \mathbf{u}_o^i / 2 - \omega^i| \right] := \frac{T^i}{I^i} \\ \frac{dr^i}{dt} = 0, & \frac{dh^i}{dt} = 0, \end{cases} \quad (3.1)$$

where we assume that the floe sizes and thicknesses do not change in time. In what follows, we adopt BBGKY hierarchy (Bogoliubov–Born–Green–Kirkwood–Yvon, [8–10, 50, 70]) to derive a kinetic equation for the one-particle distribution function over the generalized phase space $\mathbb{R}_x^2 \times \mathbb{R}_v^2 \times \mathbb{T} \times \mathbb{R}_\omega \times \mathbb{R}_+ \times \mathbb{R}_+$ (\mathbb{T} means 1D torus). In general, one assumes that the distribution function belongs to a function class such that it is periodic in the toroidal variables and rapidly decaying in the unbounded variables, ensuring that all boundary terms arising from integration by parts vanish.

• Step A (Derivation of the Liouville equation for the n -particle distribution function): First, we define n -particle distribution function on the n -particle phase space $\mathbb{R}^{4n} \times \mathbb{T}^n \times \mathbb{R}^n \times \mathbb{R}_+^{2n}$:

$$F^n = F^n(t, \mathbf{x}^1, \mathbf{v}^1, \theta^1, \omega^1, r^1, h^1, \dots, \mathbf{x}^n, \mathbf{v}^n, \theta^n, \omega^n, r^n, h^n), \quad (3.2)$$

for $(\mathbf{x}^i, \mathbf{v}^i, \theta^i, \omega^i, r^i, h^i) \in \mathbb{R}^2 \times \mathbb{R}^2 \times \mathbb{T} \times \mathbb{R}_\omega \times \mathbb{R}_+ \times \mathbb{R}_+, i \in [n]$.

Note that the n -particle probability density function F^n is symmetric in its phase variable in the sense that

$$\begin{aligned} F^n(t, \dots, \mathbf{x}^i, \mathbf{v}^i, \theta^i, \omega^i, r^i, h^i, \dots, \mathbf{x}^j, \mathbf{v}^j, \theta^j, \omega^j, r^j, h^j, \dots) \\ = F^n(t, \dots, \mathbf{x}^j, \mathbf{v}^j, \theta^j, \omega^j, r^j, h^j, \dots, \mathbf{x}^i, \mathbf{v}^i, \theta^i, \omega^i, r^i, h^i, \dots). \end{aligned} \quad (3.3)$$

Then, F^n satisfies the Liouville equation on the generalized n -particle phase space:

$$\begin{aligned} \partial_t F^n + \sum_{i=1}^n \nabla_{\mathbf{x}^i} \cdot (\dot{\mathbf{x}}^i F^n) + \sum_{i=1}^n \nabla_{\mathbf{v}^i} \cdot (\dot{\mathbf{v}}^i F^n) \\ + \sum_{i=1}^n \partial_{\theta^i} (\dot{\theta}^i F^n) + \sum_{i=1}^n \partial_{\omega^i} (\dot{\omega}^i F^n) + \sum_{i=1}^n \partial_{r^i} (\dot{r}^i F^n) + \sum_{i=1}^n \partial_{h^i} (\dot{h}^i F^n) = 0, \end{aligned} \quad (3.4)$$

where $\nabla_{\mathbf{x}^i} \cdot (\)$ and $\nabla_{\mathbf{v}^i} \cdot (\)$ denote the divergences in \mathbf{x}^i and \mathbf{v}^i -variables, respectively. By using (3.1), the above system can also be written as

$$\partial_t F^n + \sum_{i=1}^n \mathbf{v}^i \cdot \nabla_{\mathbf{x}^i} F^n + \sum_{i=1}^n \nabla_{\mathbf{v}^i} \cdot \left(\frac{\mathbf{F}^i}{m^i} F^n \right) + \sum_{i=1}^n \omega^i \partial_{\theta^i} F^n + \sum_{i=1}^n \partial_{\omega^i} \left(\frac{T^i}{I^i} F^n \right) = 0. \quad (3.5)$$

• Step B (Derivation of equation for the j -particle distribution function): For notational simplicity, we set

$$z := (\mathbf{x}, \mathbf{v}, \theta, \omega, r, h), \quad dz^j = d\mathbf{x}^j d\mathbf{v}^j d\theta^j d\omega^j dr^j dh^j, \quad j \in [n], \quad dE^{n:j} = \prod_{i=j+1}^n dz^i.$$

Then, we introduce the j -marginal distribution function $F^{n:j}$ by the integration of (3.2):

$$F^{n:j} := \int_{\mathbb{R}^{4(n-j)} \times \mathbb{T}^{n-j} \times \mathbb{R}^{n-j} \times \mathbb{R}_+^{2(n-j)}} F^n dE^{n:j}.$$

Next, we derive an equation for $F^{n:j}$. For this, we rewrite (3.5) as follows.

$$\begin{aligned} \partial_t F^n &= - \sum_{i=1}^j \nabla_{\mathbf{x}^i} \cdot (\mathbf{v}^i F^n) - \sum_{i=1}^j \nabla_{\mathbf{v}^i} \cdot \left(\frac{\mathbf{F}^i}{m^i} F^n \right) - \sum_{i=1}^j \partial_{\theta^i} (\omega^i F^n) - \sum_{i=1}^j \partial_{\omega^i} \left(\frac{T^i}{I^i} F^n \right) \\ &\quad - \sum_{i=j+1}^n \nabla_{\mathbf{x}^i} \cdot (\mathbf{v}^i F^n) - \sum_{i=j+1}^n \nabla_{\mathbf{v}^i} \cdot \left(\frac{\mathbf{F}^i}{m^i} F^n \right) - \sum_{i=j+1}^n \partial_{\theta^i} (\omega^i F^n) - \sum_{i=j+1}^n \partial_{\omega^i} \left(\frac{T^i}{I^i} F^n \right). \end{aligned} \quad (3.6)$$

Now, set $\hat{\mathbb{R}} = \mathbb{R}^{4(n-j)} \times \mathbb{T}^{n-j} \times \mathbb{R}^{n-j} \times \mathbb{R}_+^{2(n-j)}$, and integrate the Liouville equation (3.6) over $E^{n:j}$ to obtain

$$\begin{aligned} \partial_t F^{n:j} &= - \sum_{i=1}^j \int_{\hat{\mathbb{R}}} \nabla_{\mathbf{x}^i} \cdot (\mathbf{v}^i F^n) dE^{n:j} - \sum_{i=1}^j \int_{\hat{\mathbb{R}}} \nabla_{\mathbf{v}^i} \cdot \left(\frac{\mathbf{F}^i}{m^i} F^n \right) dE^{n:j} \\ &\quad - \sum_{i=1}^j \int_{\hat{\mathbb{R}}} \partial_{\theta^i} (\omega^i F^n) dE^{n:j} - \sum_{i=1}^j \int_{\hat{\mathbb{R}}} \partial_{\omega^i} \left(\frac{T^i}{I^i} F^n \right) dE^{n:j} \\ &\quad - \sum_{i=j+1}^n \int_{\hat{\mathbb{R}}} \nabla_{\mathbf{x}^i} \cdot (\mathbf{v}^i F^n) dE^{n:j} - \sum_{i=j+1}^n \int_{\hat{\mathbb{R}}} \nabla_{\mathbf{v}^i} \cdot \left(\frac{\mathbf{F}^i}{m^i} F^n \right) dE^{n:j} \quad (3.7) \\ &\quad - \sum_{i=j+1}^n \int_{\hat{\mathbb{R}}} \partial_{\theta^i} (\omega^i F^n) dE^{n:j} - \sum_{i=j+1}^n \int_{\hat{\mathbb{R}}} \partial_{\omega^i} \left(\frac{T^i}{I^i} F^n \right) dE^{n:j} \\ &=: \sum_{k=1}^8 \mathcal{T}_{3k}. \end{aligned}$$

Using the divergence theorem and the decay condition of F^n at infinity, it is easy to verify the following identities:

$$\mathcal{T}_{3k} = 0, \quad k = 5, 6, 7, 8.$$

In the next lemma, we estimate the terms \mathcal{T}_{3i} , $i = 1, \dots, 4$, one by one. For simplicity, we denote $\hat{\mathbb{R}}_1 = \mathbb{R}^4 \times \mathbb{T} \times \mathbb{R} \times \mathbb{R}_+^2$.

Lemma 3.1. *Let F^n be a global solution to (3.4) which decays to zero sufficiently fast at infinity for all phase variables. Then, we have the following identities:*

$$\begin{aligned}
(i) \quad \mathcal{T}_{31} &= -\sum_{i=1}^j \mathbf{v}^i \cdot \nabla_{\mathbf{x}^i} F^{n:j}, \quad \mathcal{T}_{33} = -\sum_{i=1}^j \omega^i \partial_{\theta^i} F^{n:j}, \\
(ii) \quad \mathcal{T}_{32} &= -\frac{1}{n} \sum_{i=1}^j \nabla_{\mathbf{v}^i} \cdot \left[\left(\frac{1}{m^i} \sum_{k=1}^j \mathbf{f}_c^{ik} \right) F^{n:j} \right] - \frac{n-j}{n} \sum_{i=1}^j \int_{\hat{\mathbb{R}}_1} \nabla_{\mathbf{v}^i} \cdot \left(\frac{1}{m^i} \mathbf{f}_c^{i(j+1)} F^{n:j+1} \right) d\mathbf{z}^{j+1} \\
&\quad - \sum_{i=1}^j \frac{1}{m^i} \nabla_{\mathbf{v}^i} \cdot \left(\alpha^i (\mathbf{u}_o^i - \mathbf{v}^i) |\mathbf{u}_o^i - \mathbf{v}^i| F^{n:j} \right), \\
(iii) \quad \mathcal{T}_{34} &= -\frac{1}{n} \sum_{i=1}^j \partial_{\omega^i} \left(\frac{F^{n:j}}{I^i} \sum_{k=1}^j (r^i \mathbf{n}^{ik} \times \mathbf{f}_t^{ik}) \right) \\
&\quad - \frac{n-j}{n} \sum_{i=1}^j \int_{\hat{\mathbb{R}}_1} \partial_{\omega^i} \left(\frac{F^{n:j+1}}{I^i} (r^i \mathbf{n}^{i(j+1)} \times \mathbf{f}_t^{i(j+1)}) \right) d\mathbf{z}^{j+1} \\
&\quad - \sum_{i=1}^j \frac{1}{I^i} \partial_{\omega^i} \left(\beta^i (\nabla \times \mathbf{u}_o^i / 2 - \omega^i) |\nabla \times \mathbf{u}_o^i / 2 - \omega^i| F^{n:j} \right).
\end{aligned}$$

Proof. (i) With variable independence, we exchange the derivative and integration to arrive at

$$\mathcal{T}_{31} = -\sum_{i=1}^j \int_{\hat{\mathbb{R}}} \nabla_{\mathbf{x}^i} \cdot (\mathbf{v}^i F^n) dE^{n:j} = -\sum_{i=1}^j \nabla_{\mathbf{x}^i} \cdot (\mathbf{v}^i F^{n:j}) = -\sum_{i=1}^j \mathbf{v}^i \cdot \nabla_{\mathbf{x}^i} F^{n:j}.$$

Similarly, we calculate

$$\mathcal{T}_{33} = -\sum_{i=1}^j \int_{\hat{\mathbb{R}}} \partial_{\theta^i} (\omega^i F^n) dE^{n:j} = -\sum_{i=1}^j \omega^i \partial_{\theta^i} F^{n:j}.$$

(ii) Now, we use (3.3) to see that

$$\begin{aligned}
\mathcal{T}_{32} &= - \sum_{i=1}^j \int_{\hat{\mathbb{R}}} \nabla_{\mathbf{v}^i} \cdot \left(\frac{\mathbf{F}^i}{m^i} F^n \right) dE^{n:j} \\
&= - \frac{1}{n} \sum_{i=1}^j \int_{\hat{\mathbb{R}}} \nabla_{\mathbf{v}^i} \cdot \left(\frac{F^n}{m^i} \sum_{k=1}^n \mathbf{f}_c^{ik} \right) dE^{n:j} \\
&\quad - \sum_{i=1}^j \frac{1}{m^i} \int_{\hat{\mathbb{R}}} \nabla_{\mathbf{v}^i} \cdot \left(\alpha^i (\mathbf{u}_o^i - \mathbf{v}^i) |\mathbf{u}_o^i - \mathbf{v}^i| F^n \right) dE^{n:j} \\
&= - \frac{1}{n} \sum_{i=1}^j \int_{\hat{\mathbb{R}}} \nabla_{\mathbf{v}^i} \cdot \left(\frac{F^n}{m^i} \sum_{k=1}^j \mathbf{f}_c^{ik} \right) dE^{n:j} - \frac{1}{n} \sum_{i=1}^j \int_{\hat{\mathbb{R}}} \nabla_{\mathbf{v}^i} \cdot \left(\frac{F^n}{m^i} \sum_{k=j+1}^n \mathbf{f}_c^{ik} \right) dE^{n:j} \\
&\quad - \sum_{i=1}^j \frac{1}{m^i} \nabla_{\mathbf{v}^i} \cdot \left(\alpha^i (\mathbf{u}_o^i - \mathbf{v}^i) |\mathbf{u}_o^i - \mathbf{v}^i| F^{n:j} \right) \\
&= - \frac{1}{n} \sum_{i=1}^j \nabla_{\mathbf{v}^i} \cdot \left[\left(\frac{1}{m^i} \sum_{k=1}^j \mathbf{f}_c^{ik} \right) F^{n:j} \right] - \frac{n-j}{n} \sum_{i=1}^j \int_{\hat{\mathbb{R}}_1} \nabla_{\mathbf{v}^i} \cdot \left(\frac{1}{m^i} \mathbf{f}_c^{i(j+1)} F^{n:j+1} \right) d\mathbf{z}^{j+1} \\
&\quad - \sum_{i=1}^j \frac{1}{m^i} \nabla_{\mathbf{v}^i} \cdot \left(\alpha^i (\mathbf{u}_o^i - \mathbf{v}^i) |\mathbf{u}_o^i - \mathbf{v}^i| F^{n:j} \right).
\end{aligned}$$

(iii) Similarly, we use (3.1), (3.3) and calculate

$$\begin{aligned}
\mathcal{T}_{34} &= - \sum_{i=1}^j \int_{\hat{\mathbb{R}}} \partial_{\omega^i} \left(\frac{T^i}{I^i} F^n \right) dE^{n:j} \\
&= - \frac{1}{n} \sum_{i=1}^j \int_{\hat{\mathbb{R}}} \partial_{\omega^i} \left(\frac{F^n}{I^i} \sum_{k=1}^n (r^i \mathbf{n}^{ik} \times \mathbf{f}_t^{ik}) \right) dE^{n:j} \\
&\quad - \sum_{i=1}^j \frac{1}{I^i} \int_{\hat{\mathbb{R}}} \partial_{\omega^i} \left(\beta^i (\nabla \times \mathbf{u}_o^i / 2 - \omega^i) |\nabla \times \mathbf{u}_o^i / 2 - \omega^i| F^n \right) dE^{n:j} \\
&= - \frac{1}{n} \sum_{i=1}^j \partial_{\omega^i} \left(\frac{F^{n:j}}{I^i} \sum_{k=1}^j (r^i \mathbf{n}^{ik} \times \mathbf{f}_t^{ik}) \right) \\
&\quad - \frac{n-j}{n} \sum_{i=1}^j \int_{\hat{\mathbb{R}}_1} \partial_{\omega^i} \left(\frac{F^{n:j+1}}{I^i} (r^i \mathbf{n}^{i(j+1)} \times \mathbf{f}_t^{i(j+1)}) \right) d\mathbf{z}^{j+1} \\
&\quad - \sum_{i=1}^j \frac{1}{I^i} \partial_{\omega^i} \left(\beta^i (\nabla \times \mathbf{u}_o^i / 2 - \omega^i) |\nabla \times \mathbf{u}_o^i / 2 - \omega^i| F^{n:j} \right).
\end{aligned}$$

□

For a fixed j , let $n \rightarrow \infty$ and we assume that there exists a limit F^j such that

$$\lim_{n \rightarrow \infty} F^{n:j} = F^j \quad \text{in suitable sense.}$$

Then, in (3.7), we use Lemma 3.1 and formally as $n \rightarrow \infty$, the limit F^j satisfies

$$\begin{aligned} \partial_t F^j &+ \sum_{i=1}^j \mathbf{v}^i \cdot \nabla_{\mathbf{x}^i} F^j + \sum_{i=1}^j \int_{\hat{\mathbb{R}}_1} \nabla_{\mathbf{v}^i} \cdot \left(\frac{1}{m^i} \mathbf{f}_c^{i(j+1)} F^{j+1} \right) d\mathbf{z}^{j+1} \\ &+ \sum_{i=1}^j \omega^i \partial_{\theta^i} F^j + \sum_{i=1}^j \int_{\hat{\mathbb{R}}_1} \partial_{\omega^i} \left(\frac{F^{j+1}}{I^i} (r^i \mathbf{n}^{i(j+1)} \times \mathbf{f}_t^{i(j+1)}) \right) d\mathbf{z}^{j+1} \\ &+ \sum_{i=1}^j \frac{1}{m^i} \nabla_{\mathbf{v}^i} \cdot \left(\alpha^i (\mathbf{u}_o^i - \mathbf{v}^i) |\mathbf{u}_o^i - \mathbf{v}^i| F^j \right) \\ &+ \sum_{i=1}^j \frac{1}{I^i} \partial_{\omega^i} \left(\beta^i (\nabla \times \mathbf{u}_o^i / 2 - \omega^i) |\nabla \times \mathbf{u}_o^i / 2 - \omega^i| F^j \right) = 0. \end{aligned} \quad (3.8)$$

Note that the dynamics of F^j in (3.8) depends on F^{j+1} . In particular, for $j = 1$, we remove the superscript for simplicity to arrive at

$$\begin{aligned} \partial_t F + \mathbf{v} \cdot \nabla_{\mathbf{x}} F + \omega \partial_{\theta} F + \frac{\alpha}{m} \nabla_{\mathbf{v}} \cdot \left((\mathbf{u}_o - \mathbf{v}) |\mathbf{u}_o - \mathbf{v}| F \right) \\ + \frac{\beta}{I} \partial_{\omega} \left((\nabla \times \mathbf{u}_o / 2 - \omega) |\nabla \times \mathbf{u}_o / 2 - \omega| F \right) \\ + \int_{\hat{\mathbb{R}}_1} \nabla_{\mathbf{v}} \cdot \left(\frac{1}{m} \mathbf{f}_c^{12} F^2 \right) d\mathbf{z}^2 + \int_{\hat{\mathbb{R}}_1} \partial_{\omega} \left(\frac{F^2}{I} (r \mathbf{n}^{12} \times \mathbf{f}_t^{12}) \right) d\mathbf{z}^2 = 0. \end{aligned} \quad (3.9)$$

• Step C (Formal derivation of kinetic equation for one-particle distribution function): We assume the “molecular chaos assumption” by setting

$$F^2(t, \mathbf{z}, \mathbf{z}^*) = F(t, \mathbf{z}) \otimes F(t, \mathbf{z}^*). \quad (3.10)$$

Finally, we substitute the ansatz (3.10) into (3.9) to get the kinetic equation for F :

$$\begin{aligned} \partial_t F + \mathbf{v} \cdot \nabla_{\mathbf{x}} F + \omega \partial_{\theta} F + \frac{\alpha}{m} \nabla_{\mathbf{v}} \cdot \left((\mathbf{u}_o - \mathbf{v}) |\mathbf{u}_o - \mathbf{v}| F \right) \\ + \frac{\beta}{I} \partial_{\omega} \left((\nabla \times \mathbf{u}_o / 2 - \omega) |\nabla \times \mathbf{u}_o / 2 - \omega| F \right) + \nabla_{\mathbf{v}} \cdot \left[\left(\int_{\hat{\mathbb{R}}_1} \frac{1}{m} \mathbf{f}_c^{12} F(t, \mathbf{z}^*) d\mathbf{z}^* \right) F(t, \mathbf{z}) \right] \\ + \partial_{\omega} \left[\left(\int_{\hat{\mathbb{R}}_1} \frac{1}{I} (r \mathbf{n}^{12} \times \mathbf{f}_t^{12}) F(t, \mathbf{z}^*) d\mathbf{z}^* \right) F(t, \mathbf{z}) \right] = 0. \end{aligned} \quad (3.11)$$

In what follows, we use handy notation:

$$\begin{aligned}
\gamma_o &:= \frac{\alpha}{m}, & \gamma_b &:= \frac{\beta}{I}, & \gamma_1 &:= \frac{\kappa_1}{m}, & \gamma_2 &:= \frac{\kappa_2}{m}, & \gamma_3 &:= \frac{\zeta\kappa_3}{m}, & \gamma_4 &:= \frac{\zeta\kappa_3}{I}, \\
\mathbf{f}[F] &= \mathbf{f}_o + \mathbf{f}_c[F], & \mathbf{f}_o &:= \gamma_o(\mathbf{u}_o - \mathbf{v})|\mathbf{u}_o - \mathbf{v}|, & \mathbf{f}_c[F] &= \mathbf{f}_{c,n}[F] + \mathbf{f}_{c,v}[F] + \mathbf{f}_{c,t}[F], \\
\mathbf{f}_{c,n}[F](t, \mathbf{z}) &:= \int_{\hat{\mathbb{R}}_1} \gamma_1(|\mathbf{x}^* - \mathbf{x}| - (r + r^*))\mathbf{n}(\mathbf{x}, \mathbf{x}^*)F(t, \mathbf{z}^*)d\mathbf{z}^*, \\
\mathbf{f}_{c,v}[F](t, \mathbf{z}) &:= \int_{\hat{\mathbb{R}}_1} \gamma_2[(\mathbf{v} - \mathbf{v}^*) \cdot \mathbf{n}(\mathbf{x}, \mathbf{x}^*)]\mathbf{n}(\mathbf{x}, \mathbf{x}^*)F(t, \mathbf{z}^*)d\mathbf{z}^*, \\
\mathbf{f}_{c,t}[F](t, \mathbf{z}) &:= \int_{\hat{\mathbb{R}}_1} \gamma_3\sigma\mathbf{t}(\mathbf{x}, \mathbf{x}^*)F(t, \mathbf{z}^*)d\mathbf{z}^*, \\
f_\omega[F] &= f_{\omega,o}[F] + f_{\omega,t}[F], & f_{\omega,o}[F] &= \gamma_b(\nabla \times \mathbf{u}_o/2 - \omega)|\nabla \times \mathbf{u}_o/2 - \omega|, \\
f_{\omega,t}[F](t, \mathbf{z}) &:= \int_{\hat{\mathbb{R}}_1} \gamma_4 r \sigma F(t, \mathbf{z}^*)d\mathbf{z}^*,
\end{aligned} \tag{3.12}$$

where the last integration used $\mathbf{n}(\mathbf{x}, \mathbf{x}^*) \times \mathbf{t}(\mathbf{x}, \mathbf{x}^*) = 1$. Note that γ_i are all functions of the phase variables (r, h, r^*, h^*) . Finally, we substitute (3.12) into (3.11) to arrive at the Vlasov-McKean equation:

$$\partial_t F + \mathbf{v} \cdot \nabla_{\mathbf{x}} F + \omega \partial_\theta F + \nabla_{\mathbf{v}} \cdot (\mathbf{f}[F]F) + \partial_\omega (f_\omega[F]F) = 0. \tag{3.13}$$

We remark that the final two terms on the left-hand side of (3.13) account for the internal stress within the floe field due to contact interactions and the external forcing from ocean drag.

3.2 Macroscopic behavior of the kinetic model

From now on, as long as there is no confusion, we suppress t -dependence in F . i.e.,

$$F(\mathbf{z}) \equiv F(t, \mathbf{z}), \quad \mathbf{z} \in \hat{\mathbb{R}}_1.$$

For simplicity, we denote $\hat{\mathbb{R}}_2 = \mathbb{R}^8 \times \mathbb{T}^2 \times \mathbb{R}^2 \times \mathbb{R}_+^4$. Next, we define the energy functional as follows.

$$\begin{cases}
\mathcal{E} := \mathcal{E}_K + \mathcal{E}_P + \mathcal{E}_\omega, \\
\mathcal{E}_K := \frac{1}{2} \int_{\hat{\mathbb{R}}_1} m|\mathbf{v}|^2 F(\mathbf{z})d\mathbf{z}, & \mathcal{E}_\omega := \frac{1}{2} \int_{\hat{\mathbb{R}}_1} I\omega^2 F(\mathbf{z})d\mathbf{z}, \\
\mathcal{E}_P := \frac{1}{2} \int_{\hat{\mathbb{R}}_2} \left(\int_0^{\delta(\mathbf{z}, \mathbf{z}^*)} \tilde{\kappa}_1(\eta)\eta d\eta \right) F(\mathbf{z})F(\mathbf{z}^*)d\mathbf{z}d\mathbf{z}^*, & \tilde{\kappa}_1(\delta(\mathbf{z}, \mathbf{z}^*)) = \kappa_1(\mathbf{z}, \mathbf{z}^*).
\end{cases}$$

We observe that each functional component in \mathcal{E} is nonnegative, hence the energy functional \mathcal{E} is nonnegative. In the following two lemmas, we establish the macroscopic behavior of the kinetic description of the floe dynamics.

Lemma 3.2 (Macroscopic behavior). *Let F be a global smooth probability density solution to system (3.13) which decays sufficiently fast at infinity in phase space. Then, the following estimates hold.*

$$\begin{aligned}
(i) \quad & \frac{d}{dt} \int_{\hat{\mathbb{R}}_1} mF(t, \mathbf{z}) d\mathbf{z} = 0. \\
(ii) \quad & \frac{d}{dt} \int_{\hat{\mathbb{R}}_1} m\mathbf{v}F d\mathbf{z} = \int_{\hat{\mathbb{R}}_1} \alpha(\mathbf{u}_o - \mathbf{v}) |\mathbf{u}_o - \mathbf{v}| F(t, \mathbf{z}) d\mathbf{z}. \\
(iii) \quad & \frac{d}{dt} \int_{\hat{\mathbb{R}}_1} (m\mathbf{x} \times \mathbf{v} + I\omega)F d\mathbf{z} = \int_{\hat{\mathbb{R}}_1} \alpha \mathbf{x} \times (\mathbf{u}_o - \mathbf{v}) |\mathbf{u}_o - \mathbf{v}| F(t, \mathbf{z}) d\mathbf{z} \\
& \quad + \int_{\hat{\mathbb{R}}_1} \beta (\nabla \times \mathbf{u}_o/2 - \omega) |\nabla \times \mathbf{u}_o/2 - \omega| F(t, \mathbf{z}) d\mathbf{z}. \\
(iv) \quad & \frac{d\mathcal{E}}{dt} = \int_{\hat{\mathbb{R}}_1} \alpha \mathbf{v} \cdot (\mathbf{u}_o - \mathbf{v}) |\mathbf{u}_o - \mathbf{v}| F(\mathbf{z}) d\mathbf{z} \\
& \quad + \int_{\hat{\mathbb{R}}_1} \beta \omega (\nabla \times \mathbf{u}_o/2 - \omega) |\nabla \times \mathbf{u}_o/2 - \omega| F(t, \mathbf{z}) d\mathbf{z} \\
& \quad + \frac{1}{2} \int_{\hat{\mathbb{R}}_2} \kappa_2 [(\mathbf{v} - \mathbf{v}^*) \cdot \mathbf{n}(\mathbf{x}, \mathbf{x}^*)]^2 F(\mathbf{z}) F(\mathbf{z}^*) d\mathbf{z}^* d\mathbf{z} \\
& \quad - \frac{1}{2} \int_{\hat{\mathbb{R}}_2} \zeta \kappa_3 t_c \sigma_t^2 F(\mathbf{z}) F(\mathbf{z}^*) d\mathbf{z}^* d\mathbf{z}.
\end{aligned} \tag{3.14}$$

Proof. (i) Note that $\frac{dr}{dt} = \frac{dh}{dt} = 0$ which implies $\frac{dm}{dt} = 0$. We multiply (3.13) by m and integrate it over the phase space $\hat{\mathbb{R}}_1$ and use the decay of F at infinity to find the conservation of total mass:

$$\frac{d}{dt} \int_{\hat{\mathbb{R}}_1} mF(t, \mathbf{z}) d\mathbf{z} = 0.$$

(ii) Next, we derive a balance law for momentum. For this, we multiply (3.13) by \mathbf{v} to see that

$$\partial_t(\mathbf{v}F) + \nabla_{\mathbf{x}} \cdot (\mathbf{v} \otimes \mathbf{v}F) + \nabla_{\mathbf{v}} \cdot (\mathbf{v} \otimes \mathbf{f}[F]F) + \partial_{\theta}(\omega \mathbf{v}F) + \partial_{\omega}(\mathbf{v}f_{\omega}[F]F) = \mathbf{f}_o F + \mathbf{f}_c[F]F. \tag{3.15}$$

Similarly, using anti-symmetry, we multiply (3.15) by m and integrate it over the phase space $\hat{\mathbb{R}}_1$ to find

$$\begin{aligned}
\frac{d}{dt} \int_{\hat{\mathbb{R}}_1} m\mathbf{v}F(t, \mathbf{z}) d\mathbf{z} &= \int_{\hat{\mathbb{R}}_1} m\mathbf{f}_o F d\mathbf{z} + \int_{\hat{\mathbb{R}}_1} m\mathbf{f}_c[F]F d\mathbf{z} \\
&= \int_{\hat{\mathbb{R}}_1} \alpha(\mathbf{u}_o - \mathbf{v}) |\mathbf{u}_o - \mathbf{v}| F(\mathbf{z}) d\mathbf{z} + \int_{\hat{\mathbb{R}}_2} m\mathbf{f}_c(\mathbf{z}, \mathbf{z}^*) F(\mathbf{z}^*) F(\mathbf{z}) d\mathbf{z}^* d\mathbf{z} \\
&= \int_{\hat{\mathbb{R}}_1} \alpha(\mathbf{u}_o - \mathbf{v}) |\mathbf{u}_o - \mathbf{v}| F(\mathbf{z}) d\mathbf{z} - \int_{\hat{\mathbb{R}}_2} m\mathbf{f}_c(\mathbf{z}^*, \mathbf{z}) F(\mathbf{z}^*) F(\mathbf{z}) d\mathbf{z}^* d\mathbf{z} \\
&= \int_{\hat{\mathbb{R}}_1} \alpha(\mathbf{u}_o - \mathbf{v}) |\mathbf{u}_o - \mathbf{v}| F(\mathbf{z}) d\mathbf{z}.
\end{aligned}$$

This gives the desired result.

(iii) First, using the property of cross product $\mathbf{v} \times \mathbf{v} = 0$, we multiply (3.13) by $m\mathbf{x} \times \mathbf{v}$ and integrate the resulting relation to find

$$\begin{aligned}
& \frac{d}{dt} \int_{\hat{\mathbb{R}}_1} (m\mathbf{x} \times \mathbf{v})F(t, \mathbf{z})d\mathbf{z} \\
&= - \int_{\hat{\mathbb{R}}_1} (m\mathbf{x} \times \mathbf{v})\nabla_{\mathbf{x}} \cdot (\mathbf{v}F)d\mathbf{z} - \int_{\hat{\mathbb{R}}_1} (m\mathbf{x} \times \mathbf{v})\nabla_{\mathbf{v}} \cdot (\mathbf{f}[F]F)d\mathbf{z} \\
&- \int_{\hat{\mathbb{R}}_1} \partial_{\theta}(m\omega(\mathbf{x} \times \mathbf{v})F)d\mathbf{z} - \int_{\hat{\mathbb{R}}_1} \partial_{\omega}(m(\mathbf{x} \times \mathbf{v})f_{\omega}[F]F)d\mathbf{z} \\
&= \int_{\hat{\mathbb{R}}_1} m\mathbf{v} \times \mathbf{v}Fd\mathbf{z} + \int_{\hat{\mathbb{R}}_1} m\mathbf{x} \times \mathbf{f}[F]Fd\mathbf{z} \\
&= \int_{\hat{\mathbb{R}}_1} m\mathbf{x} \times \mathbf{f}_oFd\mathbf{z} + \int_{\hat{\mathbb{R}}_1} m\mathbf{x} \times (\mathbf{f}_{c,n}[F] + \mathbf{f}_{c,v}[F] + \mathbf{f}_{c,t}[F])Fd\mathbf{z} \\
&= S_1 + S_{21} + S_{22} + S_{23}.
\end{aligned}$$

Next estimate S_1 and S_{2i} , $i = 1, 2$ one by one.

- (Estimation of S_1): We use the functional form of f_o in (3.12).

$$S_1 = \alpha \int_{\hat{\mathbb{R}}_1} \mathbf{x} \times (\mathbf{u}_o - \mathbf{v}) |\mathbf{u}_o - \mathbf{v}| F(t, \mathbf{z})d\mathbf{z}.$$

- (Estimation of S_2 , $i = 1, 2$): We use anti-symmetry of the integrand under the transformation $\mathbf{z} \leftrightarrow \mathbf{z}^*$ to get

$$\begin{aligned}
S_{21} &= \int_{\hat{\mathbb{R}}_2} m\gamma_1(|\mathbf{x}^* - \mathbf{x}| - (r + r^*)) (\mathbf{x} \times \mathbf{n}(\mathbf{x}, \mathbf{x}^*))F(t, \mathbf{z}^*)d\mathbf{z}^*d\mathbf{z} \\
&= - \int_{\hat{\mathbb{R}}_2} m\gamma_1(|\mathbf{x}^* - \mathbf{x}| - (r + r^*)) (\mathbf{x}^* \times \mathbf{n}(\mathbf{x}, \mathbf{x}^*))F(t, \mathbf{z}^*)d\mathbf{z}^*d\mathbf{z} \\
&= \frac{1}{2} \int_{\hat{\mathbb{R}}_2} m\gamma_1(|\mathbf{x}^* - \mathbf{x}| - (r + r^*)) ((\mathbf{x} - \mathbf{x}^*) \times \mathbf{n}(\mathbf{x}, \mathbf{x}^*))F(t, \mathbf{z}^*)d\mathbf{z}^*d\mathbf{z} = 0.
\end{aligned}$$

$$\begin{aligned}
S_{22} &= \int_{\hat{\mathbb{R}}_2} m\gamma_2[(\mathbf{v} - \mathbf{v}^*) \cdot \mathbf{n}(\mathbf{x}, \mathbf{x}^*)] (\mathbf{x} \times \mathbf{n}(\mathbf{x}, \mathbf{x}^*))F(t, \mathbf{z}^*)d\mathbf{z}^*d\mathbf{z} \\
&= - \int_{\hat{\mathbb{R}}_2} m\gamma_2[(\mathbf{v} - \mathbf{v}^*) \cdot \mathbf{n}(\mathbf{x}, \mathbf{x}^*)] (\mathbf{x}^* \times \mathbf{n}(\mathbf{x}, \mathbf{x}^*))F(t, \mathbf{z}^*)d\mathbf{z}^*d\mathbf{z} \\
&= \frac{1}{2} \int_{\hat{\mathbb{R}}_2} m\gamma_2[(\mathbf{v} - \mathbf{v}^*) \cdot \mathbf{n}(\mathbf{x}, \mathbf{x}^*)] ((\mathbf{x} - \mathbf{x}^*) \times \mathbf{n}(\mathbf{x}, \mathbf{x}^*))F(t, \mathbf{z}^*)d\mathbf{z}^*d\mathbf{z} = 0.
\end{aligned}$$

$$S_{23} = \int_{\hat{\mathbb{R}}_2} m(\mathbf{x} \times \mathbf{f}_{c,t}[F])F(t, \mathbf{z}^*)d\mathbf{z}^*d\mathbf{z}$$

Next, we calculate the spin angular part to get

$$\begin{aligned}
\frac{d}{dt} \int_{\hat{\mathbb{R}}_1} I\omega F(t, \mathbf{z}) d\mathbf{z} &= -\frac{1}{2} \int_{\hat{\mathbb{R}}_1} \nabla_{\mathbf{x}} \cdot (I\omega \mathbf{v}F) d\mathbf{z} - \int_{\hat{\mathbb{R}}_1} \nabla_{\mathbf{v}} \cdot (I\omega \mathbf{f}[F]F) d\mathbf{z} \\
&\quad - \int_{\hat{\mathbb{R}}_1} \partial_{\theta}(I\omega^2 F) d\mathbf{z} - \int_{\hat{\mathbb{R}}_1} I\omega \partial_{\omega}(f_{\omega}[F]F) d\mathbf{z} \\
&= \int_{\hat{\mathbb{R}}_1} I(f_{\omega,o}[F] + f_{\omega,t}[F])F d\mathbf{z} \\
&= S_3 + S_4,
\end{aligned}$$

where

$$S_3 = \int_{\hat{\mathbb{R}}_1} I\gamma_b (\nabla \times \mathbf{u}_o/2 - \omega) |\nabla \times \mathbf{u}_o/2 - \omega| F(t, \mathbf{z}) d\mathbf{z}.$$

Following the same argument as in (2.13), we combine S_{23} and S_4 to calculate

$$S_{23} + S_4 = \int_{\hat{\mathbb{R}}_2} m(\mathbf{c} \times \mathbf{f}_{c,t}[F])F(t, \mathbf{z}^*) d\mathbf{z}^* d\mathbf{z} = 0.$$

This leads to the desired result by summing up the above terms.

(iv) We multiply $\frac{1}{2}|\mathbf{v}|^2$ to (3.13) and $\frac{1}{2}\omega^2$ to (3.13) to get

$$\begin{aligned}
\partial_t \left(\frac{1}{2} |\mathbf{v}|^2 F \right) + \nabla_{\mathbf{x}} \cdot \left(\frac{1}{2} |\mathbf{v}|^2 \mathbf{v} F \right) + \nabla_{\mathbf{v}} \cdot \left(\frac{1}{2} |\mathbf{v}|^2 \mathbf{f}[F] F \right) + \partial_{\theta}(\omega |\mathbf{v}|^2 F)/2 + \partial_{\omega}(|\mathbf{v}|^2 f_{\omega}[F] F)/2 \\
= (\mathbf{v} \cdot \mathbf{f}_o) F + (\mathbf{v} \cdot \mathbf{f}_c[F]) F, \\
\partial_t \left(\frac{1}{2} \omega^2 F \right) + \nabla_{\mathbf{x}} \cdot \left(\frac{\omega^2}{2} \mathbf{v} F \right) + \nabla_{\mathbf{v}} \cdot \left(\frac{\omega^2}{2} \mathbf{f}[F] F \right) + \partial_{\theta}(\omega^3 F)/2 + \partial_{\omega}(\omega^2 f_{\omega}[F] F)/2 \\
= (\omega f_{\omega,o}) F + (\omega f_{\omega,t}[F]) F.
\end{aligned} \tag{3.16}$$

Now, we multiply two equations in (3.16) by m and I , respectively, and integrate them over $\hat{\mathbb{R}}_1$ to find

$$\begin{aligned}
\frac{d}{dt} \int_{\hat{\mathbb{R}}_1} \frac{1}{2} m |\mathbf{v}|^2 F(\mathbf{z}) d\mathbf{z} &= \int_{\hat{\mathbb{R}}_1} m(\mathbf{v} \cdot \mathbf{f}_o) F(\mathbf{z}) d\mathbf{z} + \int_{\hat{\mathbb{R}}_1} m(\mathbf{v} \cdot \mathbf{f}_c[F])(\mathbf{z}) F(t, \mathbf{z}) d\mathbf{z} \\
&=: \mathcal{T}_{41} + \mathcal{T}_{42} + \mathcal{T}_{43} + \mathcal{T}_{44}, \\
\frac{d}{dt} \int_{\hat{\mathbb{R}}_1} \frac{1}{2} I \omega^2 F(\mathbf{z}) d\mathbf{z} &= \int_{\hat{\mathbb{R}}_1} I(\omega f_{\omega,o}) F(\mathbf{z}) d\mathbf{z} + \int_{\hat{\mathbb{R}}_1} I(\omega f_{\omega,t}[F])(\mathbf{z}) F(t, \mathbf{z}) d\mathbf{z} \\
&=: \mathcal{T}_{45} + \mathcal{T}_{46}.
\end{aligned} \tag{3.17}$$

Below, we estimate the term \mathcal{T}_{4i} , $i = 1, 2, \dots, 6$, one by one.

• Case D.1 (Estimate of \mathcal{T}_{41} and \mathcal{T}_{45}): We use the definition of \mathbf{f}_o and $f_{\omega,o}$ in (3.12) to see

$$\begin{aligned}
\mathcal{T}_{41} &= \int_{\hat{\mathbb{R}}_1} \alpha \mathbf{v} \cdot (\mathbf{u}_o - \mathbf{v}) |\mathbf{u}_o - \mathbf{v}| F(\mathbf{z}) d\mathbf{z}, \\
\mathcal{T}_{45} &= \int_{\hat{\mathbb{R}}_1} \beta \omega (\nabla \times \mathbf{u}_o/2 - \omega) |\nabla \times \mathbf{u}_o/2 - \omega| F(t, \mathbf{z}) d\mathbf{z}.
\end{aligned} \tag{3.18}$$

- Case D.2 (Estimate of \mathcal{T}_{42}): By direct calculation, we obtain

$$\begin{aligned}
\mathcal{T}_{42} &= \int_{\hat{\mathbb{R}}_2} \kappa_1(|\mathbf{x}^* - \mathbf{x}| - (r + r^*)) \mathbf{v} \cdot \mathbf{n}(\mathbf{x}, \mathbf{x}^*) F(\mathbf{z}^*) F(\mathbf{z}) d\mathbf{z}^* d\mathbf{z} \\
&= \int_{\hat{\mathbb{R}}_2} \kappa_1(|\mathbf{x} - \mathbf{x}^*| - (r^* + r)) \mathbf{v}^* \cdot \mathbf{n}(\mathbf{x}^*, \mathbf{x}) F(\mathbf{z}) F(\mathbf{z}^*) d\mathbf{z} d\mathbf{z}^* \\
&= - \int_{\hat{\mathbb{R}}_2} \kappa_1(|\mathbf{x}^* - \mathbf{x}| - (r + r^*)) \mathbf{v}^* \cdot \mathbf{n}(\mathbf{x}, \mathbf{x}^*) F(\mathbf{z}^*) F(\mathbf{z}) d\mathbf{z}^* d\mathbf{z} \\
&= \frac{1}{2} \int_{\hat{\mathbb{R}}_2} \kappa_1(|\mathbf{x}^* - \mathbf{x}| - (r + r^*)) (\mathbf{v} - \mathbf{v}^*) \cdot \mathbf{n}(\mathbf{x}, \mathbf{x}^*) F(\mathbf{z}^*) F(\mathbf{z}) d\mathbf{z}^* d\mathbf{z} \\
&= - \frac{d\mathcal{E}_P}{dt},
\end{aligned} \tag{3.19}$$

where we used an exchange map $\mathbf{z} \longleftrightarrow \mathbf{z}^*$ and $\mathbf{n}(\mathbf{x}^*, \mathbf{x}) = -\mathbf{n}(\mathbf{x}, \mathbf{x}^*)$. We will prove the last equality. For simplicity, we set

$$p(\mathbf{z}, \mathbf{z}_*) := \int_0^{\delta(\mathbf{z}, \mathbf{z}_*)} \tilde{\kappa}_1(\eta) \eta d\eta,$$

and note that it is only dependent on \mathbf{x} , r , m , and h . Since

$$\begin{aligned}
&\partial_t(F(\mathbf{z})F(\mathbf{z}_*)) + (\mathbf{v}, \mathbf{v}_*) \cdot (\nabla_{\mathbf{x}}, \nabla_{\mathbf{x}_*})(F(\mathbf{z})F(\mathbf{z}_*)) \\
&\quad + (\omega, \omega_*) \cdot (\partial_\theta, \partial_{\theta_*})(F(\mathbf{z})F(\mathbf{z}_*)) \\
&\quad + (\nabla_{\mathbf{v}}, \nabla_{\mathbf{v}_*}) \cdot ((\mathbf{f}[F](\mathbf{z}), \mathbf{f}[F](\mathbf{z}_*))F(\mathbf{z})F(\mathbf{z}_*)) \\
&\quad + (\partial_\omega, \partial_{\omega_*}) \cdot ((f_\omega[F](\mathbf{z}), f_\omega[F](\mathbf{z}_*))F(\mathbf{z})F(\mathbf{z}_*)) = 0,
\end{aligned}$$

by integration by parts, we have

$$\begin{aligned}
\frac{d\mathcal{E}_P}{dt} &= \frac{1}{2} \int_{\hat{\mathbb{R}}_2} p(\mathbf{z}, \mathbf{z}_*) \partial_t(F(\mathbf{z})F(\mathbf{z}_*)) d\mathbf{z} d\mathbf{z}_* \\
&= - \frac{1}{2} \int_{\hat{\mathbb{R}}_2} p(\mathbf{z}, \mathbf{z}_*) (\mathbf{v}, \mathbf{v}_*) \cdot (\nabla_{\mathbf{x}}, \nabla_{\mathbf{x}_*})(F(\mathbf{z})F(\mathbf{z}_*)) d\mathbf{z} d\mathbf{z}_* \\
&= \frac{1}{2} \int_{\hat{\mathbb{R}}_2} [\nabla_{\mathbf{x}} p(\mathbf{z}, \mathbf{z}_*) \cdot \mathbf{v} + \nabla_{\mathbf{x}_*} p(\mathbf{z}, \mathbf{z}_*) \cdot \mathbf{v}_*] F(\mathbf{z}) F(\mathbf{z}_*) d\mathbf{z} d\mathbf{z}_*.
\end{aligned}$$

Note that divergence other than in \mathbf{x} , \mathbf{x}_* cancels $p(\mathbf{z}, \mathbf{z}_*)$ so that they are zero. Since $\nabla_{\mathbf{x}} p(\mathbf{z}, \mathbf{z}_*) = -\kappa_1(\mathbf{z}, \mathbf{z}_*) \delta(\mathbf{z}, \mathbf{z}_*) \mathbf{n}(\mathbf{x}, \mathbf{x}_*)$,

$$\frac{d\mathcal{E}_P}{dt} = - \frac{1}{2} \int \kappa_1 \delta(\mathbf{v} - \mathbf{v}^*) \cdot \mathbf{n}(\mathbf{x}, \mathbf{x}^*) F(\mathbf{z}^*) F(\mathbf{z}) d\mathbf{z}^* d\mathbf{z} = -\mathcal{T}_{42}.$$

- Case D.3 (Estimate of \mathcal{T}_{43}): Similar to Case D.2, we have

$$\begin{aligned}
\mathcal{T}_{43} &= \int_{\hat{\mathbb{R}}_2} m\gamma_2 [(\mathbf{v} - \mathbf{v}^*) \cdot \mathbf{n}(\mathbf{x}, \mathbf{x}^*)] \mathbf{n}(\mathbf{x}, \mathbf{x}^*) \cdot \mathbf{v} F(\mathbf{z}) F(\mathbf{z}^*) d\mathbf{z}^* d\mathbf{z} \\
&= - \int_{\hat{\mathbb{R}}_2} m\gamma_2 [(\mathbf{v} - \mathbf{v}^*) \cdot \mathbf{n}(\mathbf{x}, \mathbf{x}^*)] \mathbf{n}(\mathbf{x}, \mathbf{x}^*) \cdot \mathbf{v}^* F(\mathbf{z}) F(\mathbf{z}^*) d\mathbf{z}^* d\mathbf{z} \\
&= \frac{1}{2} \int_{\hat{\mathbb{R}}_2} \kappa_2 [(\mathbf{v} - \mathbf{v}^*) \cdot \mathbf{n}(\mathbf{x}, \mathbf{x}^*)]^2 F(\mathbf{z}) F(\mathbf{z}^*) d\mathbf{z}^* d\mathbf{z} \leq 0.
\end{aligned} \tag{3.20}$$

- Case D.4 (Estimate of $\mathcal{T}_{44} + \mathcal{T}_{46}$): Similarly, using the definition (2.2), we have

$$\begin{aligned}
\mathcal{T}_{44} + \mathcal{T}_{46} &= \int_{\hat{\mathbb{R}}_2} [m\gamma_3 \mathbf{f}_t(\mathbf{z}, \mathbf{z}^*) \cdot \mathbf{v} + I\gamma_4 r\omega \mathbf{n}(\mathbf{z}, \mathbf{z}^*) \times \mathbf{f}_t(\mathbf{z}, \mathbf{z}^*)] F(\mathbf{z}) F(\mathbf{z}^*) d\mathbf{z}^* d\mathbf{z} \\
&= \int_{\hat{\mathbb{R}}_2} [\mathbf{f}_t(\mathbf{z}, \mathbf{z}^*) \cdot \mathbf{v} + r\omega \mathbf{n}(\mathbf{z}, \mathbf{z}^*) \times \mathbf{f}_t(\mathbf{z}, \mathbf{z}^*)] F(\mathbf{z}) F(\mathbf{z}^*) d\mathbf{z}^* d\mathbf{z} \\
&= \int_{\hat{\mathbb{R}}_2} [-\mathbf{f}_t(\mathbf{z}, \mathbf{z}^*) \cdot \mathbf{v}^* + r^* \omega^* \mathbf{n}(\mathbf{z}, \mathbf{z}^*) \times \mathbf{f}_t(\mathbf{z}, \mathbf{z}^*)] F(\mathbf{z}) F(\mathbf{z}^*) d\mathbf{z}^* d\mathbf{z} \\
&= \frac{1}{2} \int_{\hat{\mathbb{R}}_2} [(\mathbf{f}_t(\mathbf{z}, \mathbf{z}^*) \cdot \mathbf{t}(\mathbf{z}, \mathbf{z}^*)) \mathbf{t}(\mathbf{z}, \mathbf{z}^*) \cdot (\mathbf{v} - \mathbf{v}^*) \\
&\quad + (r\omega + r^* \omega^*) (\mathbf{f}_t(\mathbf{z}, \mathbf{z}^*) \cdot \mathbf{t}(\mathbf{z}, \mathbf{z}^*)) \mathbf{n}(\mathbf{z}, \mathbf{z}^*) \times \mathbf{t}(\mathbf{z}, \mathbf{z}^*)] F(\mathbf{z}) F(\mathbf{z}^*) d\mathbf{z}^* d\mathbf{z} \\
&= -\frac{1}{2} \int_{\hat{\mathbb{R}}_2} (\mathbf{f}_t \cdot \mathbf{t}) [(\mathbf{v}^* - \mathbf{v}) \cdot \mathbf{t} - r\omega - r^* \omega^*] F(\mathbf{z}) F(\mathbf{z}^*) d\mathbf{z}^* d\mathbf{z} \\
&= -\frac{1}{2} \int_{\hat{\mathbb{R}}_2} \zeta \kappa_3 t_c \sigma_t^2 F(\mathbf{z}) F(\mathbf{z}^*) d\mathbf{z}^* d\mathbf{z} \leq 0,
\end{aligned} \tag{3.21}$$

where we used anti-symmetry and

$$\mathbf{f}_t(\mathbf{z}, \mathbf{z}^*) = (\mathbf{f}_t(\mathbf{z}, \mathbf{z}^*) \cdot \mathbf{t}(\mathbf{z}, \mathbf{z}^*)) \mathbf{t}(\mathbf{z}, \mathbf{z}^*), \quad \mathbf{n}(\mathbf{z}, \mathbf{z}^*) \times \mathbf{t}(\mathbf{z}, \mathbf{z}^*) = 1.$$

In (3.17), we combine all the estimates (3.18), (3.19), (3.20) and (3.21) to get the desired estimate in (3.14). \square

We remark that the above result tells that in the case of no ocean drag, i.e., $\alpha^i = \beta^i = 0$, the energy is dissipative since $\kappa_2 < 0$.

Theorem 3.3. *Suppose the ocean velocity is a constant \mathbf{u}_o^∞ and let $F(\mathbf{x}, \mathbf{v}, \theta, \omega, r, h)$ be a global solution to system (3.13) with a compact support bounded in an open ball. Assume that the floe radius r and thickness h are bounded from below and above once the system is initialized. Then, we have*

$$\lim_{t \rightarrow \infty} \int_{\hat{\mathbb{R}}_1} \alpha |\mathbf{u}_o^\infty - \mathbf{v}|^3 F(t, \mathbf{z}) d\mathbf{z} = 0, \quad \text{and} \quad \lim_{t \rightarrow \infty} \int_{\hat{\mathbb{R}}_1} \beta |\omega|^3 F(t, \mathbf{z}) d\mathbf{z} = 0.$$

Furthermore, if $\mathbf{u}_o^\infty = \mathbf{0}$, then

$$\lim_{t \rightarrow \infty} \mathcal{E}_K(t) = 0, \quad \lim_{t \rightarrow \infty} \mathcal{E}_\omega(t) = 0.$$

Proof. We use the proof of Theorem 3.5 in [23] and Lemma 3.2 to find

$$\frac{d\mathcal{E}}{dt} \leq - \int_{\hat{\mathbb{R}}_1} \alpha |\mathbf{u}_o^\infty - \mathbf{v}|^3 F(\mathbf{z}) d\mathbf{z} - \int_{\hat{\mathbb{R}}_1} \beta |\omega|^3 F(t, \mathbf{z}) d\mathbf{z}, \tag{3.22}$$

since the other two terms are non-positive (noting that $\kappa_2 \leq 0$). Thus, total energy is non-increasing. Next, we integrate inequality (3.22), to get

$$\int_0^\infty \left(\int_{\hat{\mathbb{R}}_1} \alpha |\mathbf{u}_o^\infty - \mathbf{v}|^3 F(\mathbf{z}) d\mathbf{z} + \int_{\hat{\mathbb{R}}_1} \beta |\omega|^3 F(t, \mathbf{z}) d\mathbf{z} \right) dt \leq \mathcal{E}(0) - \inf_{t>0} \mathcal{E}(t) \leq \mathcal{E}(0),$$

as the total energy is non-negative. Therefore it is enough to show the uniform continuity of these two terms to prove the first claim using Barbalat's lemma. We evaluate the time-derivative of the above terms:

$$\begin{aligned}
& \int_{\hat{\mathbb{R}}_1} \alpha |\mathbf{u}_o^\infty - \mathbf{v}|^3 \partial_t F(\mathbf{z}) d\mathbf{z} \\
&= - \int_{\hat{\mathbb{R}}_1} \alpha |\mathbf{u}_o^\infty - \mathbf{v}|^3 (\mathbf{v} \cdot \nabla_{\mathbf{x}} F + \omega \partial_\theta F + \nabla_{\mathbf{v}} \cdot (\mathbf{f}[F]F) + \partial_\omega (f_\omega[F]F)) d\mathbf{z} \\
&= - \int_{\hat{\mathbb{R}}_1} \alpha |\mathbf{u}_o^\infty - \mathbf{v}|^3 \nabla_{\mathbf{v}} \cdot (\mathbf{f}[F]F) d\mathbf{z} \\
&= 3 \int_{\hat{\mathbb{R}}_1} \alpha |\mathbf{u}_o^\infty - \mathbf{v}| (\mathbf{v} - \mathbf{u}_o^\infty) \cdot (\mathbf{f}_o + \mathbf{f}_c[F]) F d\mathbf{z} := \mathcal{T}_\alpha, \\
& \int_{\hat{\mathbb{R}}_1} \beta |\omega|^3 \partial_t F(\mathbf{z}) d\mathbf{z} \\
&= - \int_{\hat{\mathbb{R}}_1} \beta |\omega|^3 (\mathbf{v} \cdot \nabla_{\mathbf{x}} F + \omega \partial_\theta F + \nabla_{\mathbf{v}} \cdot (\mathbf{f}[F]F) + \partial_\omega (f_\omega[F]F)) d\mathbf{z} \\
&= - \int_{\hat{\mathbb{R}}_1} \beta |\omega|^3 \partial_\omega (f_\omega[F]F) d\mathbf{z} \\
&= 3 \int_{\hat{\mathbb{R}}_1} \beta |\omega| \omega (f_\omega[F]F) d\mathbf{z} := \mathcal{T}_\beta,
\end{aligned}$$

where we used (3.13) and the divergence theorem with fast decay in the density function F for vanishing boundaries. The two integrals \mathcal{T}_α and \mathcal{T}_β are bounded by some time-independent constant C . We briefly check this fact. Assume that there exists a compact set $K \subset \hat{\mathbb{R}}_1$ and $r_0, h_0 > 0$ such that

$$\text{supp } F(t, \cdot) \subset K \cap \{r \geq r_0\} \cap \{h \geq h_0\} \text{ for all } t \geq 0.$$

Since K is compact, we can set

$$\bar{\alpha} := \|\alpha\|_{L^\infty(K)}, \quad \bar{\beta} := \|\beta\|_{L^\infty(K)}, \quad \bar{U} := \sup_K |u_\infty - v|, \quad \bar{\Omega} := \sup_K |\omega|.$$

Moreover, all coefficients in the force fields are bounded on $K \times K$. Using the force decomposition

$$f[F] = f_o + f_c[F] \quad \text{and} \quad f_\omega[F] = f_{\omega,o} + f_{\omega,c}[F],$$

one has

$$\|f_o\|_{L^\infty(K)} \leq \|\gamma_0\|_{L^\infty(K)} \bar{U}^2 \leq C, \quad \|f_{\omega,o}\|_{L^\infty(K)} \leq \|\gamma_\omega\|_{L^\infty(K)} \bar{\Omega}^2 \leq C.$$

For the contact terms, by compactness and mass conservation, we have

$$\begin{aligned}
\|f_{c,\mathbf{n}}[F](t, \cdot)\|_{L^\infty(K)} &\leq \|\gamma_1 \delta\|_{L^\infty(K^2)} \leq C, \\
\|f_{c,\mathbf{v}}[F](t, \cdot)\|_{L^\infty(K)} &\leq \|\gamma_2 |(\mathbf{v} - \mathbf{v}_*) \cdot \mathbf{n}|\|_{L^\infty(K^2)} \leq C.
\end{aligned}$$

The tangential part is controlled by the Coulomb cut-off $|\zeta\kappa_3\sigma| \leq \mu|\kappa_1\delta|$:

$$\|f_{c,t}[F](t, \cdot)\|_{L^\infty(K)} \leq \left\| \frac{\mu|\kappa_1\delta|}{m} \right\|_{L^\infty(K^2)} \leq C.$$

Hence

$$\|f[F](t, \cdot)\|_{L^\infty(K)} + \|f_\omega[F](t, \cdot)\|_{L^\infty(K)} \leq C \text{ uniformly in } t.$$

Therefore we have

$$|T_\alpha(t)| \leq 3\bar{\alpha}\bar{U}^2 \|f[F](t, \cdot)\|_{L^\infty(K)} \int_K F(t, \mathbf{z}) d\mathbf{z} \leq C.$$

Similarly, one has

$$|T_\beta(t)| \leq 3\bar{\beta}\bar{\Omega}^2 \|f_\omega[F](t, \cdot)\|_{L^\infty(K)} \int_K F(t, \mathbf{z}) d\mathbf{z} \leq C,$$

with a constant $C > 0$ independent of t . Thus $t \mapsto \int \alpha|u_\infty - v|^3 F$ and $t \mapsto \int \beta|\omega|^3 F$ are uniformly continuous on $[0, \infty)$. We use Barbalat's Lemma 2.6 to get the first two results. Lastly, using weighted Hölder's inequality, one can bound the translational kinetic energy as

$$\begin{aligned} \mathcal{E}_K &= \frac{1}{2} \int_{\hat{\mathbb{R}}_1} m|\mathbf{v}|^2 F(\mathbf{z}) d\mathbf{z} \\ &\leq \frac{1}{2} \left(\int_{\hat{\mathbb{R}}_1} \alpha|v|^3 F(t, \mathbf{z}) d\mathbf{z} \right)^{2/3} \left(\int_{\hat{\mathbb{R}}_1} \frac{m^3 F(t, \mathbf{z})}{\alpha^2} d\mathbf{z} \right)^{1/3} \\ &\leq C \left(\int_{\hat{\mathbb{R}}_1} \alpha|v|^3 F(t, \mathbf{z}) d\mathbf{z} \right)^{2/3}, \end{aligned}$$

where the positive constant C depends on the constants that bound the floe radius and thickness. Taking the limit $t \rightarrow \infty$ gives

$$\lim_{t \rightarrow \infty} \mathcal{E}_K = 0.$$

Similar arguments apply to estimate \mathcal{E}_ω to get the desired estimate. \square

4 From kinetic to hydrodynamic description

In this section, we derive the macroscopic (hydrodynamic) balance laws associated with the kinetic model (3.13), and then close them via a mono-kinetic ansatz.

4.1 Hydrodynamic balance laws

Throughout, we set

$$\mathbf{y} := (\mathbf{v}, \theta, \omega, r, h) \in \mathbb{R}^4 \times \mathbb{R}_+^2, \quad d\mathbf{y} := d\mathbf{v}d\theta d\omega dr dh.$$

For simplicity, we denote $\hat{\mathbb{R}}_3 = \mathbb{R}^2 \times \mathbb{T} \times \mathbb{R} \times \mathbb{R}_+^2$ and $\hat{\mathbb{R}}_4 = \mathbb{R}^4 \times \mathbb{T} \times \mathbb{R} \times \mathbb{R}_+^2$. Let $F = F(t, \mathbf{x}, \mathbf{y}) \geq 0$ be a sufficiently smooth solution of (3.13) such that F decays rapidly as $|\mathbf{v}| + |\omega| \rightarrow \infty$ and as $r + h \rightarrow \infty$, so that all integrations by parts below are justified, and boundary terms vanish.

Recall that the particle mass and moment of inertia depend on the size variables (r, h) :

$$m = m(r, h) > 0, \quad I = I(r, h) > 0.$$

From (3.1),

$$\frac{dr}{dt} = \frac{dh}{dt} = 0 \quad \implies \quad \frac{dm}{dt} = \frac{dI}{dt} = 0.$$

We define the *mass-weighted* and *inertia-weighted* local moments (hydrodynamic fields):

$$\left\{ \begin{array}{l} \rho(t, \mathbf{x}) := \int_{\hat{\mathbb{R}}_3} mF(t, \mathbf{x}, \mathbf{y}) d\mathbf{y}, \\ (\rho\mathbf{u})(t, \mathbf{x}) := \int_{\hat{\mathbb{R}}_3} m\mathbf{v}F(t, \mathbf{x}, \mathbf{y}) d\mathbf{y}, \\ \rho_I(t, \mathbf{x}) := \int_{\hat{\mathbb{R}}_3} IF(t, \mathbf{x}, \mathbf{y}) d\mathbf{y}, \\ (\rho_I\bar{\omega})(t, \mathbf{x}) := \int_{\hat{\mathbb{R}}_3} I\omega F(t, \mathbf{x}, \mathbf{y}) d\mathbf{y}, \\ \hat{\omega}(t, \mathbf{x}) := \int_{\hat{\mathbb{R}}_3} (m\mathbf{x} \times \mathbf{v} + I\omega)F(t, \mathbf{x}, \mathbf{y}) d\mathbf{y} = \mathbf{x} \times (\rho\mathbf{u}) + \rho_I\bar{\omega}, \\ E(t, \mathbf{x}) := \int_{\hat{\mathbb{R}}_3} \frac{1}{2} (m|\mathbf{v}|^2 + I\omega^2) F(t, \mathbf{x}, \mathbf{y}) d\mathbf{y}. \end{array} \right. \quad (4.1)$$

Herein, $\hat{\omega}$ denotes total angular momentum density, while $\bar{\omega}$ is the mean spin. We introduce $\mathbf{w} := \mathbf{v} - \mathbf{u}$ and the following weighted fluxes:

$$\begin{aligned} P(t, \mathbf{x}) &:= \int_{\hat{\mathbb{R}}_3} m\mathbf{w} \otimes \mathbf{w} F d\mathbf{y}, & \mathbf{q}(t, \mathbf{x}) &:= \int_{\hat{\mathbb{R}}_3} (m|\mathbf{w}|^2 + I(\omega - \bar{\omega})^2) \mathbf{w} F d\mathbf{y}, \\ \mathbf{J}(t, \mathbf{x}) &:= \int_{\hat{\mathbb{R}}_3} I(\omega - \bar{\omega}) \mathbf{w} F d\mathbf{y}, & \mathbf{J}_{\text{orb}}(t, \mathbf{x}) &:= \int_{\hat{\mathbb{R}}_3} m(\mathbf{x} \times \mathbf{w}) \otimes \mathbf{w} F(t, \mathbf{x}, \mathbf{y}) d\mathbf{y}, \end{aligned} \quad (4.2)$$

where one may omit \otimes in the definition of the orbital flux tensor \mathbf{J}_{orb} as it is 2D and $\mathbf{x} \times \mathbf{w}$ gives a scalar (we keep it here for consistency). Observe that

$$\begin{aligned} E &= E_K + E_R + E_{\text{int}}, & E_K &:= \frac{1}{2} \rho |\mathbf{u}|^2, & E_R &:= \frac{1}{2} \rho_I |\bar{\omega}|^2, \\ E_{\text{int}} &= \rho e := \frac{1}{2} \int_{\hat{\mathbb{R}}_3} (m|\mathbf{w}|^2 + I(\omega - \bar{\omega})^2) F d\mathbf{y}. \end{aligned} \quad (4.3)$$

With this setting in mind, we have the following balance laws.

Lemma 4.1 (Hydrodynamic balance laws). *Let F be a smooth solution of (3.13) with sufficient decay at infinity in \mathbf{y} . Then the moments (4.1) satisfy the local balance laws:*

$$\partial_t \rho + \nabla_{\mathbf{x}} \cdot (\rho \mathbf{u}) = 0, \quad (4.4a)$$

$$\partial_t(\rho \mathbf{u}) + \nabla_{\mathbf{x}} \cdot (\rho \mathbf{u} \otimes \mathbf{u} + P) = \int_{\hat{\mathbb{R}}_3} m \mathbf{f}[F] F d\mathbf{y}, \quad (4.4b)$$

$$\partial_t \hat{\omega} + \nabla_{\mathbf{x}} \cdot (\hat{\omega} \mathbf{u} + \mathbf{J} + \mathbf{J}_{\text{orb}}) = \int_{\hat{\mathbb{R}}_3} (m \mathbf{x} \times \mathbf{f}[F] + I f_{\omega}[F]) F d\mathbf{y}, \quad (4.4c)$$

$$\partial_t E + \nabla_{\mathbf{x}} \cdot \left(E \mathbf{u} + P \mathbf{u} + \bar{\omega} \mathbf{J} + \frac{1}{2} \mathbf{q} \right) = \int_{\hat{\mathbb{R}}_3} m \mathbf{v} \cdot \mathbf{f}[F] F d\mathbf{y} + \int_{\hat{\mathbb{R}}_3} I \omega f_{\omega}[F] F d\mathbf{y}. \quad (4.4d)$$

Proof. We establish the balance laws in several steps as follows.

Step A: (Conservation of mass): We multiply (3.13) by m and integrate the resulting relation over \mathbf{y} . Using the integration by parts in θ , \mathbf{v} and ω , one has

$$\partial_t \rho + \nabla_{\mathbf{x}} \cdot \int_{\hat{\mathbb{R}}_3} m \mathbf{v} F d\mathbf{y} = 0.$$

This is exactly (4.4a) by the definition of $\rho \mathbf{u}$.

Step B: (Balance of Momentum): Again, we multiply (3.13) by $m \mathbf{v}$ and integrate the resulting relation over \mathbf{y} to find

$$\partial_t(\rho \mathbf{u}) + \nabla_{\mathbf{x}} \cdot \int_{\hat{\mathbb{R}}_3} m \mathbf{v} \otimes \mathbf{v} F d\mathbf{y} + \int_{\hat{\mathbb{R}}_3} m \mathbf{v} \nabla_{\mathbf{v}} \cdot (\mathbf{f}[F] F) d\mathbf{y} = 0.$$

By integration by parts in \mathbf{v} (boundary term vanishes), one has

$$\int_{\hat{\mathbb{R}}_3} m \mathbf{v} \nabla_{\mathbf{v}} \cdot (\mathbf{f}[F] F) d\mathbf{y} = - \int_{\hat{\mathbb{R}}_3} m \mathbf{f}[F] F d\mathbf{y}.$$

Next, we decompose $\mathbf{v} = \mathbf{u} + \mathbf{w}$ to get

$$\int_{\hat{\mathbb{R}}_3} m \mathbf{v} \otimes \mathbf{v} F d\mathbf{y} = \int_{\hat{\mathbb{R}}_3} m (\mathbf{u} + \mathbf{w}) \otimes (\mathbf{u} + \mathbf{w}) F d\mathbf{y} = \rho \mathbf{u} \otimes \mathbf{u} + P,$$

since $\int_{\hat{\mathbb{R}}_3} m \mathbf{w} F d\mathbf{y} = 0$ by the definition of \mathbf{u} . This gives (4.4b).

Step C: (Spin angular momentum): We multiply (3.13) by $I \omega$ and integrate it over \mathbf{y} to get

$$\partial_t(\rho_I \bar{\omega}) + \nabla_{\mathbf{x}} \cdot \int_{\hat{\mathbb{R}}_3} I \omega \mathbf{v} F d\mathbf{y} + \int_{\hat{\mathbb{R}}_3} I \omega \partial_{\omega} (f_{\omega}[F] F) d\mathbf{y} = 0.$$

Integration by parts in ω yields

$$\int_{\hat{\mathbb{R}}_3} I \omega \partial_{\omega} (f_{\omega}[F] F) d\mathbf{y} = - \int_{\hat{\mathbb{R}}_3} I f_{\omega}[F] F d\mathbf{y}.$$

Moreover, we use $\mathbf{v} = \mathbf{u} + \mathbf{w}$ and $\omega = \bar{\omega} + (\omega - \bar{\omega})$ to obtain

$$\int_{\hat{\mathbb{R}}_3} I \omega \mathbf{v} F d\mathbf{y} = \int_{\hat{\mathbb{R}}_3} I (\bar{\omega} + (\omega - \bar{\omega})) (\mathbf{u} + \mathbf{w}) F d\mathbf{y} = \rho_I \bar{\omega} \mathbf{u} + \mathbf{J},$$

where we used

$$\int_{\hat{\mathbb{R}}_3} I(\omega - \bar{\omega})F d\mathbf{y} = 0, \quad \int_{\hat{\mathbb{R}}_3} I\boldsymbol{\omega}F d\mathbf{y} = 0.$$

This yields

$$\partial_t(\rho_I \bar{\omega}) + \nabla_{\mathbf{x}} \cdot (\rho_I \bar{\omega} \mathbf{u} + \mathbf{J}) = \int_{\hat{\mathbb{R}}_3} I f_{\omega}[F]F d\mathbf{y}. \quad (4.5)$$

Step D: (Orbital angular momentum): We multiply (3.13) by $m\mathbf{x} \times \mathbf{v}$ and integrate the resulting relation over \mathbf{y} term by term.

(i) *Time derivative.*

$$\int_{\hat{\mathbb{R}}_3} m(\mathbf{x} \times \mathbf{v}) \partial_t F d\mathbf{y} = \partial_t (\mathbf{x} \times (\rho \mathbf{u})).$$

(ii) *\mathbf{x} -transport.* We use

$$\mathbf{v} \cdot \nabla_{\mathbf{x}} F = \nabla_{\mathbf{x}} \cdot (\mathbf{v} F), \quad \mathbf{v} \cdot \nabla_{\mathbf{x}} (\mathbf{x} \times \mathbf{v}) = 0,$$

(since $\mathbf{v} \times \mathbf{v} = 0$), to get

$$\int_{\hat{\mathbb{R}}_3} m(\mathbf{x} \times \mathbf{v}) \mathbf{v} \cdot \nabla_{\mathbf{x}} F d\mathbf{y} = \nabla_{\mathbf{x}} \cdot \left(\int_{\hat{\mathbb{R}}_3} m(\mathbf{x} \times \mathbf{v}) \otimes \mathbf{v} F d\mathbf{y} \right) = \nabla_{\mathbf{x}} \cdot (\mathbf{x} \times (\rho \mathbf{u}) \otimes \mathbf{u} + \mathbf{J}_{\text{orb}}),$$

where the mixed terms vanish as before.

(iii) *\mathbf{v} -divergence term.* Assuming sufficient decay in \mathbf{v} , so boundary terms vanish,

$$\int_{\hat{\mathbb{R}}_3} m(\mathbf{x} \times \mathbf{v}) \nabla_{\mathbf{v}} \cdot (\mathbf{f}[F]F) d\mathbf{y} = - \int_{\hat{\mathbb{R}}_3} m(\nabla_{\mathbf{v}}(\mathbf{x} \times \mathbf{v})) \cdot \mathbf{f}[F]F d\mathbf{y} = - \int_{\hat{\mathbb{R}}_3} m\mathbf{x} \times \mathbf{f}[F]F d\mathbf{y}.$$

The θ -transport and ω -flux terms vanish by using integration by parts. Collecting (i)–(iii), we obtain the local orbital angular momentum balance:

$$\partial_t (\mathbf{x} \times (\rho \mathbf{u})) + \nabla_{\mathbf{x}} \cdot (\mathbf{x} \times (\rho \mathbf{u}) \otimes \mathbf{u} + \mathbf{J}_{\text{orb}}) = \int_{\hat{\mathbb{R}}_3} m\mathbf{x} \times \mathbf{f}[F]F d\mathbf{y}. \quad (4.6)$$

Finally, summing up the spin and orbital angular momentum balances (4.5) and (4.6) to arrive at the desired balance law for total angular momentum (4.4c).

Step E: (Total translational and rotational energy): We multiply (3.13) by $\frac{1}{2}(m|\mathbf{v}|^2 + I\omega^2)$ and integrate the resulting relation over \mathbf{y} . The transport terms give

$$\partial_t E + \nabla_{\mathbf{x}} \cdot \int_{\hat{\mathbb{R}}_3} \frac{1}{2}(m|\mathbf{v}|^2 + I\omega^2)\mathbf{v}F d\mathbf{y},$$

and the θ -term vanishes by integration by parts. For the force terms, we use integration by parts in \mathbf{v} and ω (the mixed terms vanish using integration by parts) to see

$$\int_{\hat{\mathbb{R}}_3} \frac{1}{2}m|\mathbf{v}|^2 \nabla_{\mathbf{v}} \cdot (\mathbf{f}[F]F) d\mathbf{y} = - \int_{\hat{\mathbb{R}}_3} m\mathbf{v} \cdot \mathbf{f}[F]F d\mathbf{y},$$

$$\int_{\hat{\mathbb{R}}_3} \frac{1}{2} I \omega^2 \partial_\omega (f_\omega[F]F) d\mathbf{y} = - \int_{\hat{\mathbb{R}}_3} I \omega f_\omega[F]F d\mathbf{y}.$$

Finally, we decompose the energy flux, use $\mathbf{v} = \mathbf{u} + \mathbf{w}$ and $\omega = \bar{\omega} + (\omega - \bar{\omega})$ to obtain

$$\int_{\hat{\mathbb{R}}_3} \frac{1}{2} (m|\mathbf{v}|^2 + I\omega^2) \mathbf{v}F d\mathbf{y} = E\mathbf{u} + P\mathbf{u} + \bar{\omega}\mathbf{J} + \frac{1}{2}\mathbf{q},$$

where $P, \mathbf{J}, \mathbf{q}$ are defined in (4.2)–(4.3) and we used

$$\int_{\hat{\mathbb{R}}_3} m\mathbf{w}F d\mathbf{y} = 0, \quad \int_{\hat{\mathbb{R}}_3} I(\omega - \bar{\omega})F d\mathbf{y} = 0.$$

Finally, we collect all the estimates to get the desired estimate. \square

To close (4.4), we follow [23, 28] and adopt the mono-kinetic ansatz

$$F(t, \mathbf{x}, \mathbf{v}, \theta, \omega, r, h) = \frac{\rho(t, \mathbf{x})}{m(r, h)} \Phi(t, \mathbf{x}, \theta, r, h) \delta(\mathbf{v} - \mathbf{u}(t, \mathbf{x})) \delta(\omega - \bar{\omega}(t, \mathbf{x})), \quad (4.7)$$

where $\Phi \geq 0$ and

$$\int_{\mathbb{R} \times \mathbb{R}_+^2} \Phi(t, \mathbf{x}, \theta, r, h) dr dh d\theta = 1, \quad \text{for all } (t, \mathbf{x}). \quad (4.8)$$

Under (4.7) and (4.8), the weighted definitions are consistent:

$$\int mF d\mathbf{y} = \rho, \quad \int m\mathbf{v}F d\mathbf{y} = \rho\mathbf{u}, \quad \rho_I(t, \mathbf{x}) = \rho(t, \mathbf{x}) \int_{\mathbb{R}_+^2} \frac{I(r, h)}{m(r, h)} \Phi(t, \mathbf{x}, r, h) dr dh,$$

$$\int_{\hat{\mathbb{R}}_3} I\omega F(t, \mathbf{x}, \mathbf{y}) d\mathbf{y} = \rho(t, \mathbf{x}) \bar{\omega} \int_{\mathbb{R}_+^2} \frac{I(r, h)}{m(r, h)} \Phi(t, \mathbf{x}, r, h) dr dh = \rho_I \bar{\omega}$$

With this in mind, using (4.7) and following [23] (Dirac delta function property), one arrives at

$$P \equiv 0, \quad \mathbf{q} \equiv 0, \quad \mathbf{J} \equiv 0, \quad \mathbf{J}_{\text{orb}} \equiv 0, \quad \rho e \equiv 0,$$

and the energy reduces to the bulk form

$$E(t, \mathbf{x}) = \frac{1}{2} \rho(t, \mathbf{x}) |\mathbf{u}(t, \mathbf{x})|^2 + \frac{1}{2} \rho_I(t, \mathbf{x}) \bar{\omega}(t, \mathbf{x})^2.$$

Then the balance laws (4.4) reduce to

$$\partial_t \rho + \nabla_{\mathbf{x}} \cdot (\rho\mathbf{u}) = 0, \quad (4.9a)$$

$$\partial_t (\rho\mathbf{u}) + \nabla_{\mathbf{x}} \cdot (\rho\mathbf{u} \otimes \mathbf{u}) = \int_{\hat{\mathbb{R}}_3} m\mathbf{f}[F]F d\mathbf{y}, \quad (4.9b)$$

$$\partial_t \hat{\omega} + \nabla_{\mathbf{x}} \cdot (\hat{\omega}\mathbf{u}) = \mathbf{x} \times \int_{\hat{\mathbb{R}}_3} m\mathbf{f}[F]F d\mathbf{y} + \int_{\hat{\mathbb{R}}_3} I f_\omega[F]F d\mathbf{y}, \quad (4.9c)$$

$$\partial_t E + \nabla_{\mathbf{x}} \cdot (E\mathbf{u}) = \mathbf{u} \cdot \int_{\hat{\mathbb{R}}_3} m\mathbf{f}[F]F d\mathbf{y} + \bar{\omega} \int_{\hat{\mathbb{R}}_3} I f_{\omega}[F]F d\mathbf{y}. \quad (4.9d)$$

Now mainly using the definition (4.1) and the mono-kinetic ansatz (4.7), we evaluate the right-hand side integrals one by one below.

$$\int_{\hat{\mathbb{R}}_3} m\mathbf{f}[F]F d\mathbf{y} = \int_{\hat{\mathbb{R}}_3} m(\mathbf{f}_o + \mathbf{f}_{c,n}[F] + \mathbf{f}_{c,v}[F] + \mathbf{f}_{c,t}[F])F d\mathbf{y} := \sum_{j=1}^4 \mathcal{T}_{5j}, \quad (4.10)$$

$$\int_{\hat{\mathbb{R}}_3} I f_{\omega}[F]F d\mathbf{y} = \int_{\hat{\mathbb{R}}_3} I(\mathbf{f}_{\omega,o} + \mathbf{f}_{\omega,t}[F])F d\mathbf{y} := \mathcal{T}_{55} + \mathcal{T}_{56}. \quad (4.11)$$

(a) For ocean-drag induced terms \mathcal{T}_{51} and \mathcal{T}_{55} , we have

$$\int_{\hat{\mathbb{R}}_3} m\mathbf{f}_o F d\mathbf{y} = \bar{\alpha}(\mathbf{u}_o - \mathbf{u})|\mathbf{u}_o - \mathbf{u}|, \quad (4.12)$$

$$\int_{\hat{\mathbb{R}}_3} I f_{\omega,o} F d\mathbf{y} = \bar{\beta} \left(\frac{\nabla \times \mathbf{u}_o}{2} - \bar{\omega} \right) \left| \frac{\nabla \times \mathbf{u}_o}{2} - \bar{\omega} \right|, \quad (4.13)$$

where

$$\bar{\alpha} = \int_{\hat{\mathbb{R}}_3} \alpha F d\mathbf{y}, \quad \text{and} \quad \bar{\beta} = \int_{\hat{\mathbb{R}}_3} \beta F d\mathbf{y}.$$

(b) For \mathcal{T}_{52} , by definition (3.12), we have

$$\int_{\hat{\mathbb{R}}_3} m\mathbf{f}_{c,n}[F]F d\mathbf{y} = \int_{\hat{\mathbb{R}}_3} \int_{\hat{\mathbb{R}}_4} \kappa_1(|\mathbf{x}^* - \mathbf{x}| - (r + r^*))\mathbf{n}(\mathbf{x}, \mathbf{x}^*)F(t, \mathbf{z}^*)d\mathbf{z}^*F d\mathbf{y}. \quad (4.14)$$

This term \mathcal{T}_{52} is generally non-zero over \mathbf{x} pointwise due to the lack of integration over \mathbf{x} that induces anti-symmetry of pair forces (see Lemma 3.2 on how this term vanishes when integration over \mathbf{x} is included). If imposing the local homogeneity assumption (a strong assumption inspired by the kinetic theory of gas particles [3, 30, 31]; c.f., Appendix A), this term reduces to zero. Other terms vanish similarly, i.e., $\mathcal{T}_{53} = \mathbf{0}$, $\mathcal{T}_{54} = \mathbf{0}$ and $\mathbf{x} \times \mathcal{T}_{54} + \mathcal{T}_{56} = 0$. In this case, using (4.12), (4.13) and the above setting, the first three balance laws in (4.4) or (4.9) further reduce to

$$\partial_t \rho + \nabla_{\mathbf{x}} \cdot (\rho\mathbf{u}) = 0, \quad (4.15a)$$

$$\partial_t (\rho\mathbf{u}) + \nabla_{\mathbf{x}} \cdot (\rho\mathbf{u} \otimes \mathbf{u}) = \bar{\alpha}(\mathbf{u}_o - \mathbf{u})|\mathbf{u}_o - \mathbf{u}|, \quad (4.15b)$$

$$\partial_t \hat{\omega} + \nabla_{\mathbf{x}} \cdot (\hat{\omega}\mathbf{u}) = \bar{\alpha}\mathbf{x} \times (\mathbf{u}_o - \mathbf{u})|\mathbf{u}_o - \mathbf{u}| + \bar{\beta} \left(\frac{\nabla \times \mathbf{u}_o}{2} - \bar{\omega} \right) \left| \frac{\nabla \times \mathbf{u}_o}{2} - \bar{\omega} \right|, \quad (4.15c)$$

Remark 4.2 (Contact operator). The main difference between (4.9) and (4.15) is that the right-hand side term in (4.9) includes the contact operator acting on the phase variables that are to be integrated in the distribution sense. The right-hand side terms in (4.15b) and (4.15c) are ocean-drag induced forcing terms. The local homogeneity assumption resembles the assumption on the contact operator so that the physical laws of mass, momentum and energy conservation during collisions are satisfied (c.f., [3, Eq.

(4)] and [13, 25, 30–32, 62] among many for gas particles). This assumption on contact operator allows the simplification of the right-hand side terms in (4.15). This represents an idealized simplification of sea ice floe dynamics. In more realistic sea ice rheology, the contact-forcing terms in the density functionals generate the contact stress tensor within the ice cover. We refer to [27, 39, 63] for discussions of sea ice rheology and to Appendix A for further details.

4.2 Total energy for the closed system

We now analyze the energy dissipation properties of the closed system (4.9). We consider the more general case of (4.9) instead of (4.15) since the total energies are defined as integrals over \mathbf{x} , which implies vanishing right-hand side terms in (4.9b) and (4.9c). We first define the energies:

$$\begin{cases} \mathcal{E} := \mathcal{E}_K + \mathcal{E}_\omega + \mathcal{E}_P, \\ \mathcal{E}_K := \frac{1}{2} \int_{\mathbb{R}^2} \rho |\mathbf{u}|^2 d\mathbf{x}, & \mathcal{E}_\omega := \frac{1}{2} \int_{\mathbb{R}^2} \rho_I \bar{\omega}^2 d\mathbf{x}, \\ \mathcal{E}_P := \frac{1}{2} \int_{\mathbb{R}^4} \left[\int_{\hat{\mathbb{R}}_3^2} F F^* \left(\int_0^{\delta(\mathbf{x}, \mathbf{x}^*, r, r^*)} \kappa_1(\eta) \eta d\eta \right) \mathbf{y} d\mathbf{y}^* \right] d\mathbf{x} d\mathbf{x}^*, \end{cases} \quad (4.16)$$

where F^* denotes the density function in dual variables. Following [23], we have the following results.

Lemma 4.3 (Kinetic and rotational energy). *Let $(\rho, \mathbf{u}, \hat{\omega}, E)$ be a global smooth solution to system (4.9). Then the following holds*

$$\begin{aligned} \frac{d\mathcal{E}}{dt} &= \bar{\alpha} \int_{\mathbb{R}^2} \mathbf{u} \cdot (\mathbf{u}_o - \mathbf{u}) |\mathbf{u}_o - \mathbf{u}| d\mathbf{x} \\ &+ \bar{\beta} \int_{\mathbb{R}^2} \bar{\omega} \left(\frac{\nabla \times \mathbf{u}_o}{2} - \bar{\omega} \right) \left| \frac{\nabla \times \mathbf{u}_o}{2} - \bar{\omega} \right| d\mathbf{x} \\ &+ \frac{1}{2} \int_{\hat{\mathbb{R}}_2} \kappa_2 [(\mathbf{u} - \mathbf{u}^*) \cdot \mathbf{n}(\mathbf{x}, \mathbf{x}^*)]^2 F(\mathbf{z}) F(\mathbf{z}^*) d\mathbf{z}^* d\mathbf{z} \\ &- \frac{1}{2} \int_{\hat{\mathbb{R}}_2} \zeta \kappa_3 [(\mathbf{u}^* - \mathbf{u}) \cdot \mathbf{t} - r\bar{\omega} - r^*\bar{\omega}^*]^2 F(\mathbf{z}) F(\mathbf{z}^*) d\mathbf{z}^* d\mathbf{z}. \end{aligned}$$

Proof. We integrate (4.9d) over \mathbb{R}^2 for \mathbf{x} term-by-term.

(i) *Time derivative.* We apply the definitions (4.1) and (4.16) and the mono-kinetic ansatz (4.7) to compute

$$\int_{\mathbb{R}^2} \partial_t E d\mathbf{x} = \partial_t \int_{\mathbb{R}^2} \int_{\hat{\mathbb{R}}_3} \frac{1}{2} (m|\mathbf{v}|^2 + I\omega^2) F(t, \mathbf{x}, \mathbf{y}) d\mathbf{y} d\mathbf{x} = \frac{d}{dt} (\mathcal{E}_K + \mathcal{E}_\omega).$$

(ii) *\mathbf{x} -transport.* Using divergence theorem with vanishing boundaries gives

$$\int_{\mathbb{R}^2} \nabla_{\mathbf{x}} \cdot (E\mathbf{u}) d\mathbf{x} = 0.$$

(iii) *Right-hand side term.* The calculation follows the calculation of the integrals in (4.10) and (4.11) with further integration over \mathbb{R}^2 for \mathbf{x} . First, we use (4.12) and (4.13), to see that

$$\begin{aligned}\int_{\mathbb{R}^2} \mathbf{u} \cdot \int_{\hat{\mathbb{R}}_3} m \mathbf{f}_o F d\mathbf{y} d\mathbf{x} &= \bar{\alpha} \int_{\mathbb{R}^2} \mathbf{u} \cdot (\mathbf{u}_o - \mathbf{u}) |\mathbf{u}_o - \mathbf{u}| d\mathbf{x}, \\ \int_{\mathbb{R}^2} \bar{\omega} \int_{\hat{\mathbb{R}}_3} I f_{\omega,o} F d\mathbf{y} d\mathbf{x} &= \bar{\beta} \int_{\mathbb{R}^2} \bar{\omega} \left(\frac{\nabla \times \mathbf{u}_o}{2} - \bar{\omega} \right) \left| \frac{\nabla \times \mathbf{u}_o}{2} - \bar{\omega} \right| d\mathbf{x}.\end{aligned}$$

Secondly, for the normal contact force term (the term corresponding to \mathcal{T}_{52} in (4.14)), using the mono-kinetic ansatz (4.7), we integrate it over \mathbb{R}^2 for \mathbf{x} to arrive at

$$\begin{aligned}\int_{\mathbb{R}^2} \mathbf{u} \cdot \int_{\hat{\mathbb{R}}_3} m \mathbf{f}_{c,n}[F] F d\mathbf{y} d\mathbf{x} &= \int_{\mathbb{R}^2} \mathbf{u} \cdot \int_{\hat{\mathbb{R}}_3} \int_{\hat{\mathbb{R}}_4} \kappa_1 (|\mathbf{x}^* - \mathbf{x}| - (r + r^*)) \mathbf{n}(\mathbf{x}, \mathbf{x}^*) F(t, \mathbf{z}^*) F d\mathbf{z}^* F d\mathbf{y} d\mathbf{x} \\ &= \int_{\hat{\mathbb{R}}_4} \int_{\hat{\mathbb{R}}_4} \kappa_1 \mathbf{u} \cdot (|\mathbf{x}^* - \mathbf{x}| - (r + r^*)) \mathbf{n}(\mathbf{x}, \mathbf{x}^*) F(t, \mathbf{z}^*) F d\mathbf{z} \\ &= \int_{\hat{\mathbb{R}}_2} \kappa_1 (\mathbf{u} - \mathbf{v} + \mathbf{v}) \cdot (|\mathbf{x}^* - \mathbf{x}| - (r + r^*)) \mathbf{n}(\mathbf{x}, \mathbf{x}^*) F(t, \mathbf{z}^*) F d\mathbf{z} \\ &= \int_{\hat{\mathbb{R}}_2} \kappa_1 \mathbf{v} \cdot (|\mathbf{x}^* - \mathbf{x}| - (r + r^*)) \mathbf{n}(\mathbf{x}, \mathbf{x}^*) F(t, \mathbf{z}^*) F d\mathbf{z} \\ &= -\frac{d\mathcal{E}_P}{dt},\end{aligned}$$

where the last equality follows (3.19). Thirdly, for the damping term, we evaluate the integral in a similar fashion:

$$\begin{aligned}\int_{\mathbb{R}^2} \mathbf{u} \cdot \int_{\hat{\mathbb{R}}_3} m \mathbf{f}_{c,v}[F] F d\mathbf{y} d\mathbf{x} &= \int_{\mathbb{R}^2} \mathbf{u} \cdot \int_{\hat{\mathbb{R}}_3} \int_{\hat{\mathbb{R}}_4} \kappa_2 [(\mathbf{v} - \mathbf{v}^*) \cdot \mathbf{n}(\mathbf{x}, \mathbf{x}^*)] \mathbf{n}(\mathbf{x}, \mathbf{x}^*) F(t, \mathbf{z}^*) F d\mathbf{y} d\mathbf{x} \\ &= \int_{\hat{\mathbb{R}}_2} \kappa_2 \mathbf{u} \cdot [(\mathbf{u} - \mathbf{u}^*) \cdot \mathbf{n}(\mathbf{x}, \mathbf{x}^*)] \mathbf{n}(\mathbf{x}, \mathbf{x}^*) F(t, \mathbf{z}^*) F d\mathbf{z} \\ &= \frac{1}{2} \int_{\hat{\mathbb{R}}_2} \kappa_2 [(\mathbf{u} - \mathbf{u}^*) \cdot \mathbf{n}(\mathbf{x}, \mathbf{x}^*)]^2 F(\mathbf{z}) F(\mathbf{z}^*) d\mathbf{z}^* d\mathbf{z},\end{aligned}$$

where the last equality follows from (3.20). Lastly, we combine the last two integrals to arrive at a similar estimate as (3.21):

$$\begin{aligned}\int_{\mathbb{R}^2} \mathbf{u} \cdot \int_{\hat{\mathbb{R}}_3} m \mathbf{f}_{c,t}[F] F d\mathbf{y} d\mathbf{x} + \int_{\mathbb{R}^2} \bar{\omega} \int_{\hat{\mathbb{R}}_3} I f_{\omega,t}[F] F d\mathbf{y} d\mathbf{x} &= \int_{\hat{\mathbb{R}}_2} \zeta \kappa_3 [\mathbf{u} \cdot \sigma \mathbf{t}(\mathbf{z}, \mathbf{z}^*) + r \bar{\omega} \mathbf{n}(\mathbf{z}, \mathbf{z}^*) \times \sigma \mathbf{t}(\mathbf{z}, \mathbf{z}^*)] F(\mathbf{z}) F(\mathbf{z}^*) d\mathbf{z}^* d\mathbf{z}\end{aligned}$$

$$\begin{aligned}
&= \int_{\hat{\mathbb{R}}_2} \zeta \kappa_3 \sigma [\mathbf{u} \cdot \mathbf{t}(\mathbf{z}, \mathbf{z}^*) + r\bar{\omega}] F(\mathbf{z}) F(\mathbf{z}^*) d\mathbf{z}^* d\mathbf{z} \\
&= \int_{\hat{\mathbb{R}}_2} \zeta \kappa_3 \sigma [-\mathbf{u}^* \cdot \mathbf{t}(\mathbf{z}, \mathbf{z}^*) + r^* \bar{\omega}^*] F(\mathbf{z}) F(\mathbf{z}^*) d\mathbf{z}^* d\mathbf{z} \\
&= -\frac{1}{2} \int_{\hat{\mathbb{R}}_2} \zeta \kappa_3 \sigma [(\mathbf{u}^* - \mathbf{u}) \cdot \mathbf{t} - r\bar{\omega} - r^* \bar{\omega}^*] F(\mathbf{z}) F(\mathbf{z}^*) d\mathbf{z}^* d\mathbf{z} \\
&= -\frac{1}{2} \int_{\hat{\mathbb{R}}_2} \zeta \kappa_3 [(\mathbf{u}^* - \mathbf{u}) \cdot \mathbf{t} - r\bar{\omega} - r^* \bar{\omega}^*]^2 F(\mathbf{z}) F(\mathbf{z}^*) d\mathbf{z}^* d\mathbf{z}.
\end{aligned}$$

Summing up the estimates above and moving $-\frac{d\mathcal{E}_P}{dt}$ to the right-hand side gives the desired result. \square

Lastly, we consider two cases for ocean drag forces as an analogy in the particle and kinetic descriptions in Sections 2 and 3.

- Case A: When the ocean-drag-induced energy is removed, the total energy estimate in Lemma 4.3 implies energy dissipation:

$$\begin{aligned}
\frac{d\mathcal{E}}{dt} &= \frac{1}{2} \int_{\hat{\mathbb{R}}_2} \kappa_2 [(\mathbf{u} - \mathbf{u}^*) \cdot \mathbf{n}(\mathbf{x}, \mathbf{x}^*)]^2 F(\mathbf{z}) F(\mathbf{z}^*) d\mathbf{z}^* d\mathbf{z} \\
&\quad - \frac{1}{2} \int_{\hat{\mathbb{R}}_2} \zeta \kappa_3 [(\mathbf{u}^* - \mathbf{u}) \cdot \mathbf{t} - r\bar{\omega} - r^* \bar{\omega}^*]^2 F(\mathbf{z}) F(\mathbf{z}^*) d\mathbf{z}^* d\mathbf{z} \leq 0,
\end{aligned}$$

where the last inequality is a result of the fact that $\kappa_2 < 0$ and $\zeta \kappa_3 > 0$.

- Case B: When the ocean force is constant $\mathbf{u}_o = \mathbf{u}_o^\infty$, one expects similar velocity alignments as Theorem 2.7 for the particle model, and Theorem 3.3 for the kinetic model. In particular, $\mathbf{u}_o^\infty = \mathbf{0}$ also implies total energy dissipation, and one can follow the proof of Theorem 4.3 of [23] to establish

$$\lim_{t \rightarrow \infty} \mathcal{E}_K(t) = 0, \quad \lim_{t \rightarrow \infty} \mathcal{E}_\omega(t) = 0.$$

5 Numerical simulations

The main purpose of the numerical experiments is twofold. First, we verify the energy dissipation of the particle model, with the role of the velocity-dependent normal contact term $\mathbf{f}_{c,v}$ in producing dissipation of the total energy. In the simulations, we track the translational kinetic energy, the rotational kinetic energy, and the contact potential energy, and confirm that the total energy is dissipated due to collisions, in agreement with the analytical energy estimates derived in Section 2 (see results in Subsection 5.1). Second, we investigate the consistency between the particle and continuum descriptions by comparing ensemble-averaged particle quantities with the corresponding solutions of the hydrodynamic system, thereby validating the particle-kinetic-hydrodynamic hierarchy developed in this work (see results in Subsection 5.2). For this goal, we apply the widely-used forward Euler scheme [12, 37] to discretize (2.1) and (4.15) in time and the finite

element method [22, 44] to discretize (4.15) in space. These methods are widely used, and we omit the details of the implementation of the numerical methods for simplicity.

5.1 Example 1: Floes under constant ocean forcing

We solve the particle model (2.1) in a two-dimensional square domain. $\Omega := [-\pi, \pi]^2$ with doubly periodic boundary conditions. The prescribed ocean surface velocity is constant:

$$\mathbf{u}_o(x, y) = (0.3, 0)^T,$$

which implies $\nabla \times \mathbf{u}_o = 0$. We generate $n = 100$ floes. The radii satisfy

$$r^i \in [r_{\min}, r_{\max}], \quad r_{\min} = 0.08, \quad r_{\max} = 0.32,$$

and are sampled from a power-law distribution with exponent 2, i.e. the density is proportional to $(r^i)^{-2}$ on $[r_{\min}, r_{\max}]$. The thicknesses are sampled independently and uniformly:

$$h^i \sim \text{Unif}[0.5, 2].$$

The ice density is fixed to be $\rho_{\text{ice}} = 1$, so that $m^i = \rho_{\text{ice}}\pi(r^i)^2 h^i$, $I^i = m^i(r^i)^2$. The initial positions $\mathbf{x}^i(0)$ are sampled uniformly in Ω and accepted only if the configuration is non-overlapping in the periodic metric:

$$|\mathbf{x}^j(0) - \mathbf{x}^i(0)| \geq r^i + r^j, \quad \forall i \neq j.$$

The initial velocities and angular velocities are sampled as

$$\mathbf{v}^i(0) = (0.2 + 0.2\text{randn}, 0.2\text{randn})^T, \quad \omega^i(0) = 0.1 + 0.3\text{randn},$$

independently for each i , where randn denotes a random number following the standard Gaussian distribution $\mathcal{N}(0, 1)$. We use the physical parameters specified in Section 2.1:

$$\rho_{\text{ice}} = 1, \quad e_r = 0.15, \quad \mu^{ij} \equiv 0.2, \quad E = 10^4, \quad \nu = 0.7,$$

and compute the effective moduli E_e and G_e via (2.3). The damping parameter η is computed from (2.6). For the ocean-induced forcing coefficients in (2.2), we set $D^i = 0.9h^i$ and take $\rho_o = 1$, $C_{v,o} = 2$ and $C_{h,o} = 4$ to be $\mathcal{O}(1)$ constants (dimensionless scaling) so that the quadratic drag produces clear relaxation to the ocean velocity on the time interval $[0, 10]$. We use the forward Euler method for (2.1) with final time $T = 10$ and time step size $\Delta t = 10^{-3}$, i.e. $N_t = 10^4$ steps. During the simulation, we compute the following global observables:

- Total momentum:

$$M_{1,\mathbf{v}}(t) := \sum_{i=1}^n m^i \mathbf{v}^i(t).$$

- Total angular momentum (orbital + spin):

$$L_z(t) := \sum_{i=1}^n (\mathbf{x}^i(t) \times m^i \mathbf{v}^i(t)) \cdot \hat{\mathbf{z}} + \sum_{i=1}^n I^i \omega^i(t).$$

- Translational and rotational kinetic energies:

$$KE_t(t) := \frac{1}{2} \sum_{i=1}^n m^i |\mathbf{v}^i(t)|^2, \quad KE_r(t) := \frac{1}{2} \sum_{i=1}^n I^i |\omega^i(t)|^2.$$

- Total normal elastic strain energy (stored in the Hertz-type normal law):

$$U_n(t) := \sum_{1 \leq i < j \leq n} \frac{1}{2} \kappa_1^{ij}(t) (\delta^{ij}(t))^2 \chi^{ij}(t),$$

where δ^{ij} , κ_1^{ij} and χ^{ij} are defined in (2.2) and (2.4), and the pairwise distance d^{ij} entering δ^{ij} is computed using the periodic minimum-image convention.

We additionally track the mean velocity $\langle \mathbf{v} \rangle(t) := \frac{1}{n} \sum_{i=1}^n \mathbf{v}^i(t)$ and the mean mismatch $\frac{1}{n} \sum_{i=1}^n |\mathbf{v}^i(t) - \mathbf{u}_o^i|$ to quantify convergence to the ocean drift. Similarly, we use $\langle \omega \rangle(t)$ to denote the mean angular velocity.

In Figure 1, we can see the floe trajectories at $T = 0.001, 0.1, 1, 10$. In each subplot, the black arrows represent floe velocities \mathbf{v}^i and the floe color represents ω^i (used as a vorticity) with a fixed colorbar range $[-0.5, 0.5]$. In Figure 2, we illustrate the trajectories of the floe velocities, angular velocities, and energies. The numerical results are consistent with the long-term behavior predicted by the theory for the constant-ocean case in Theorem 2.7. In particular, we observe the following.

- *Convergence of translational velocities to the ocean velocity.* The quadratic ocean drag term in (2.1c),

$$\alpha^i (\mathbf{u}_o^i - \mathbf{v}^i) |\mathbf{u}_o^i - \mathbf{v}^i|,$$

is dissipative with respect to the relative velocity $\mathbf{v}^i - \mathbf{u}_o^i$. Numerically, we observe that the mean mismatch $\frac{1}{n} \sum_{i=1}^n |\mathbf{v}^i(t) - \mathbf{u}_o^i|$ decays in time, and the mean velocity components $\langle v_x \rangle(t)$ and $\langle v_y \rangle(t)$ approach $\mathbf{u}_{o,x} = 0.3$ and $\mathbf{u}_{o,y} = 0$. This is also reflected in the translational kinetic energy $KE_t(t)$, which approaches the kinetic energy of the drift state in which all floes move with \mathbf{u}_o :

$$KE_t(t) \longrightarrow \frac{1}{2} \sum_{i=1}^n m^i |\mathbf{u}_o|^2 \quad (t \rightarrow \infty),$$

up to small fluctuations due to intermittent collisions. In other words, $KE_t(t)$ indicates that $\mathbf{v}^i(t) \rightarrow \mathbf{u}_o^i$ in accordance with the theorem. We also observe that the collisions are less frequent, as all floe velocities align with the ocean velocity.

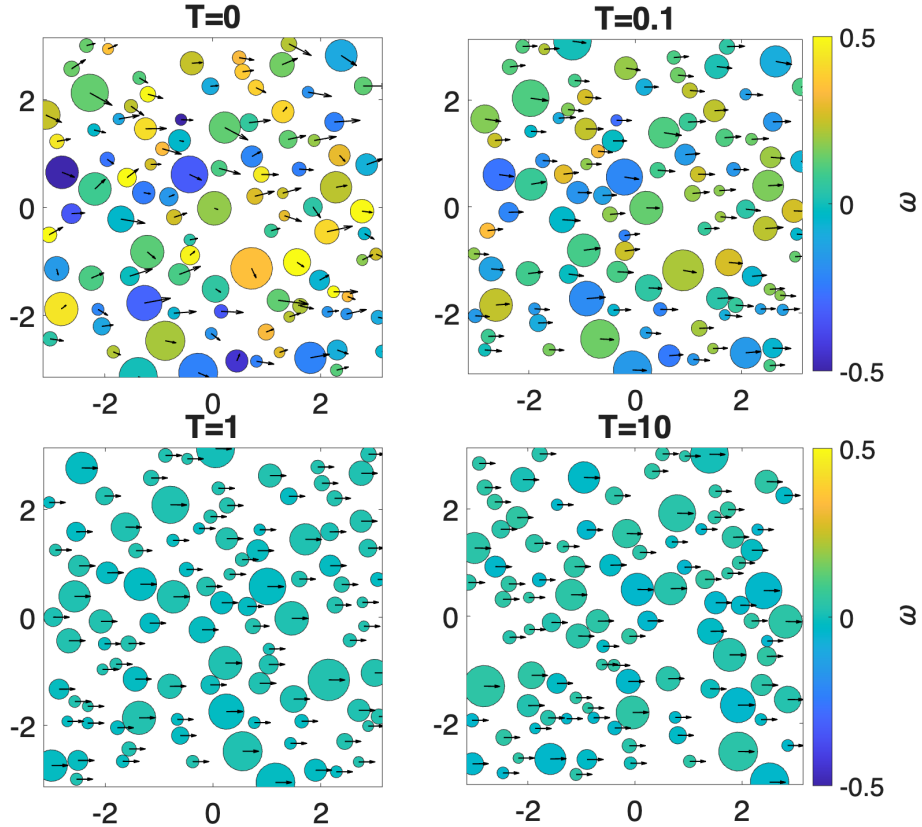


Figure 1: Example 1 floe trajectories. Arrows represent floe velocities and colors represent floe angular velocity. Ocean velocity $\mathbf{u}_o = (0.3, 0)^T$

- *Decay of angular velocity to zero.* Since $\nabla \times \mathbf{u}_o^i \equiv 0$, the quadratic rotational drag in (2.1d),

$$\beta^i \left(\nabla \times \mathbf{u}_o^i / 2 - \omega^i \right) \left| \nabla \times \mathbf{u}_o^i / 2 - \omega^i \right| = -\beta^i \omega^i |\omega^i|,$$

drives $\omega^i(t) \rightarrow 0$. Numerically, the mean angular velocity $\langle \omega \rangle(t)$ decays toward zero, and the rotational kinetic energy $KE_r(t)$ decays toward zero as well. This matches the theoretical prediction that, for a constant irrotational ocean velocity, the long-time equilibrium satisfies $\omega^i \equiv 0$.

- *Momentum balance with ocean forcing.* The contact forces satisfy action–reaction at the pair level, hence the internal forces contribute zero net momentum:

$$\sum_{i=1}^n \frac{1}{n} \sum_{j=1}^n (\mathbf{f}_n^{ij} + \mathbf{f}_t^{ij}) = \mathbf{0},$$

up to numerical error. Therefore, the evolution of $M_{1,v}(t)$ is determined solely by

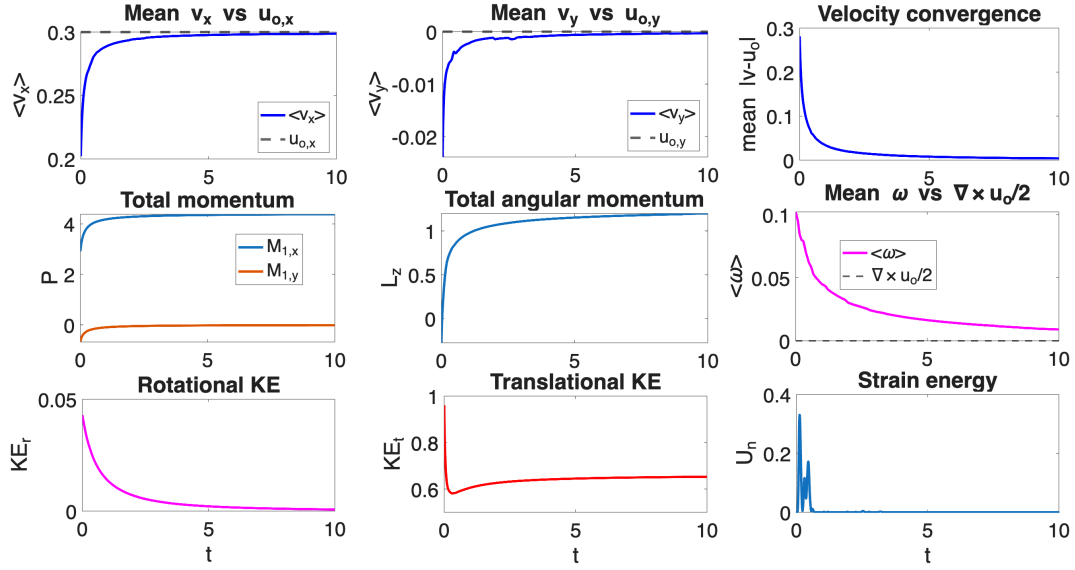


Figure 2: Example 1 floe moments. Time evolution of mean velocities, velocity differences, and angular velocities, total momentum, total angular momentum, and kinetic and normal contact strain energies.

the ocean drag (see Lemma 2.1):

$$\frac{d}{dt} M_{1,\mathbf{v}}(t) = \sum_{i=1}^n \alpha^i (\mathbf{u}_o^i - \mathbf{v}^i) |\mathbf{u}_o^i - \mathbf{v}^i|.$$

Thus $M_{1,\mathbf{v}}(t)$ is not conserved in general; instead it relaxes toward the ocean-drift momentum

$$M_{1,\mathbf{v}}^\infty := \sum_{i=1}^n m^i \mathbf{u}_o^i,$$

which is consistent with the observed convergence $\mathbf{v}^i \rightarrow \mathbf{u}_o^i$. In particular, after transients, the total momentum becomes approximately constant because $\mathbf{u}_o^i - \mathbf{v}^i \approx \mathbf{0}$ and the drag contribution becomes negligible.

- *Normal strain energy is collision-localized.* The total normal strain energy $U_n(t)$ is nonzero only during contact events (when $\chi^{ij} = 1$ and $\delta^{ij} < 0$). Numerically it appears as intermittent bursts (see the last plot in Figure 2) corresponding to collisions, and decays back toward zero when the system becomes dilute and relative motion decreases. This behavior is consistent with the short-range Hertz-type contact interaction.

5.2 Example 2: Consistency test between the particle and hydrodynamic models

This experiment is designed to test the consistency between the particle model (2.1) and the hydrodynamic (continuum) model (4.15), thereby validating the particle–kinetic–hydrodynamic hierarchy developed in this work. Unless otherwise stated, all parameters and numerical conventions are the same as in Example 1 in Subsection 5.1. We set the ocean velocity spatially varying as below:

$$\mathbf{u}_o(x, y) = (-ys, xs)^T, \quad s = \frac{(x^2 + y^2 - 4)}{32} \exp\left(-\frac{(x^2 + y^2)(x^2 + y^2 - 8)}{8}\right).$$

This choice yields a smooth rotational flow with nontrivial spatial structure and a nonzero vorticity field $\nabla \times \mathbf{u}_o$. The kinetic and hydrodynamic models are developed based on the assumption that the number of particles goes to infinity. However, it is impractical to simulate a system of a very large number of floes. For feasibility, we initialize 10,000 floes as follows. We first discretize Ω into a uniform 100×100 grid and place one floe at the center of each cell, resulting in $n = 10^4$ floes in total. All floes share the same radius and thickness, i.e., $r^i \equiv 0.02$, $h^i \equiv 1$. We set the initial translational and angular velocities to zero:

$$\mathbf{v}^i(0) = \mathbf{0}, \quad \omega^i(0) = 0, \quad i = 1, 2, \dots, 10^4.$$

The particle dynamics are evolved by the forward Euler discretization of (2.1), where the pairwise contact forces are computed using the same Hertz-type normal law and Coulomb-capped tangential law as in (2.2)–(2.5), together with the same double periodic (minimum-image) distance for contact detection.

Hydrodynamic model configuration and discretization. We solve the continuum system (4.15) for $(\rho, \mathbf{u}, \hat{\omega})$ on a uniform 50×50 grid using a linear (P_1) finite element discretization on a uniform triangulation (two triangles per square). Herein, we solve the first three equations of (4.15) for the comparison on mass density, velocity and angular velocities. Moreover, $\bar{\omega}$ is obtained from the relation $\hat{\omega} = \mathbf{x} \times (\rho \mathbf{u}) + \rho_I \bar{\omega}$ by the definition in (4.1). The time integrator is again forward Euler with $\Delta t = 10^{-3}$ and $T = 10$. With the above initialization of the particle model in mind, we prescribe the initial conditions

$$\rho(\mathbf{x}, 0) = 1, \quad \mathbf{u}(\mathbf{x}, 0) = \mathbf{0}, \quad \bar{\omega}(\mathbf{x}, 0) = \mathbf{0}.$$

We take the continuum drag coefficients $(\bar{\alpha}, \bar{\beta})$ to match the particle-level accelerations induced by the ocean forcing (using the uniform floe parameters): $\bar{\alpha} = \alpha^i$, $\bar{\beta} = \beta^i$, where α^i and β^i are defined in (2.2) (with the same choices of ρ_o , $C_{v,o}$, $C_{h,o}$ and $D^i = 0.9h^i$ as in Example 1).

Particle-to-continuum observables and comparison. For a quantitative comparison, we coarse-grain the particle data onto the same 50×50 grid used by the continuum

solver. For each coarse cell K , we compute:

$$\rho_p(K, t) := \frac{1}{|K|} \sum_{i:\mathbf{x}^i(t) \in K} m^i, \quad \mathbf{u}_p(K, t) := \frac{\sum_{i:\mathbf{x}^i(t) \in K} m^i \mathbf{v}^i(t)}{\sum_{i:\mathbf{x}^i(t) \in K} m^i}, \quad \bar{\omega}_p(K, t) := \frac{\sum_{i:\mathbf{x}^i(t) \in K} I^i \omega^i(t)}{\sum_{i:\mathbf{x}^i(t) \in K} I^i}.$$

We compare these coarse-grained particle fields with the continuum fields $(\rho, \mathbf{u}, \bar{\omega})$ at times $T = 1$ (see Figure 3) and $T = 10$ (see Figure 4) using side-by-side plots as well as cellwise differences, along with the corresponding discrete L^2 errors.

Particle vs Continuum Comparison at T=1.0

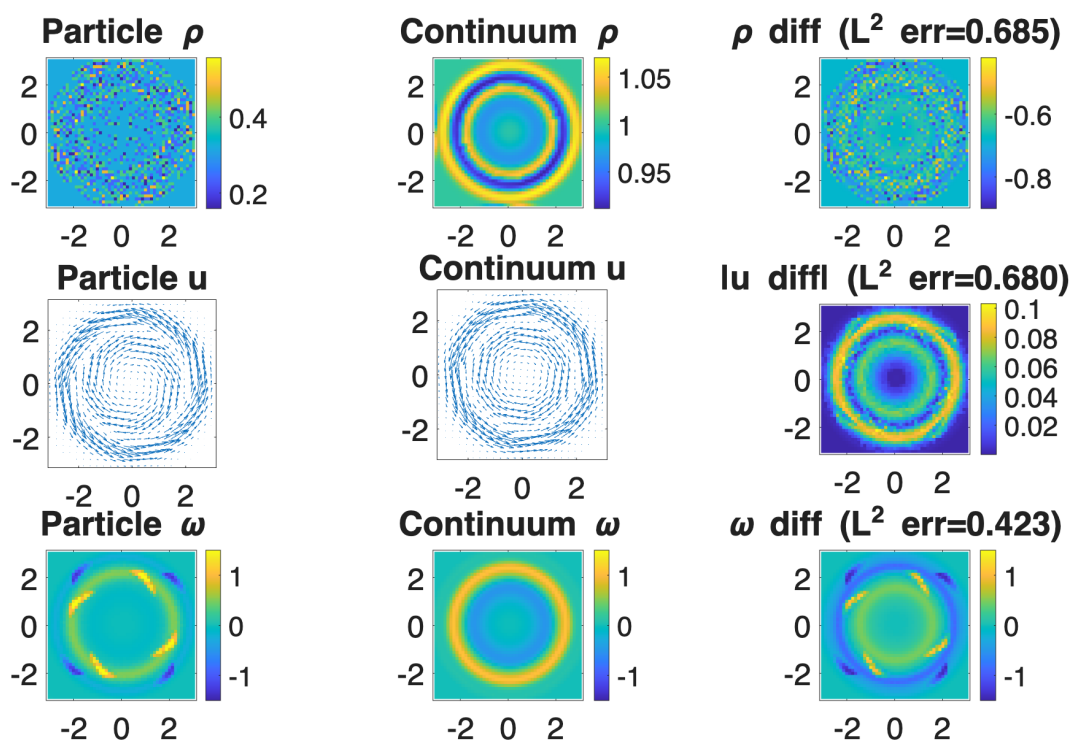


Figure 3: Model comparison at $T = 1$. Ocean velocity $\mathbf{u}_o = (-ys, xs)^T$ with $s = (x^2 + y^2 - 4)e^{-(x^2+y^2)(x^2+y^2-8)/8}/32$.

Results and discussion. The continuum solution and the coarse-grained particle statistics match well at the reported times, providing direct numerical evidence for the consistency between the particle and hydrodynamic descriptions; see Figure 3 and Figure 4. In particular, we have the following observations.

- *Mass density consistency.* Since both models start from the uniform density $\rho(\mathbf{x}, 0) = 1$ (this is scaled since a constant factor can be removed from (4.15a)). The

Particle vs Continuum Comparison at T=10.0

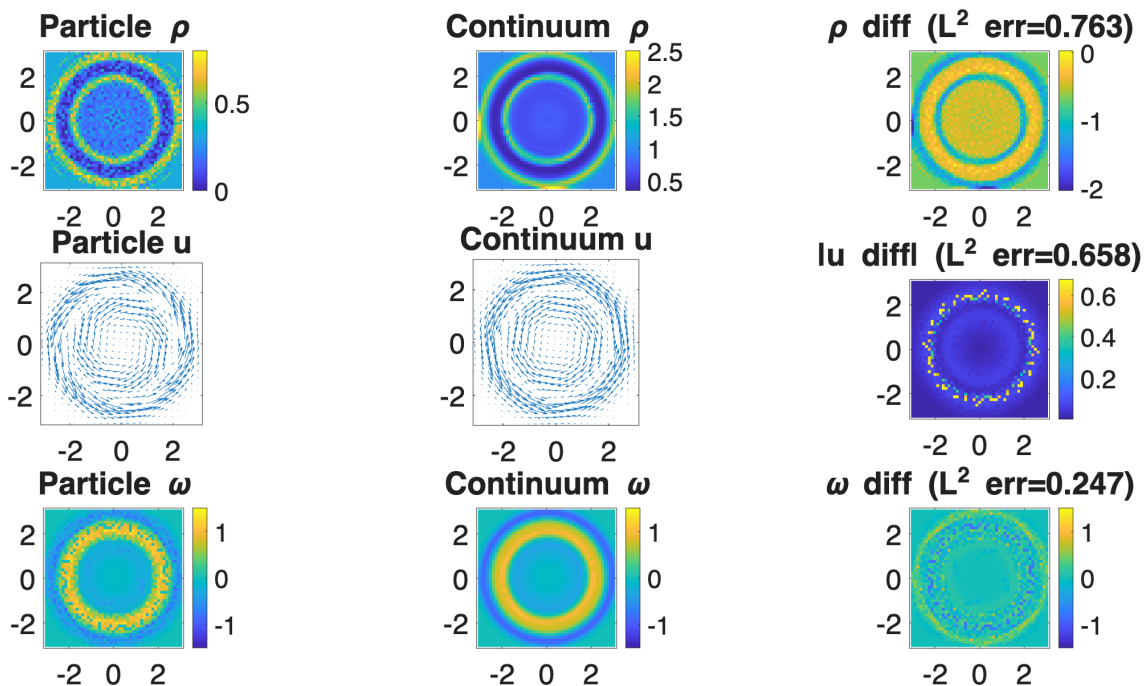


Figure 4: Model comparison at $T = 10$. Ocean velocity $\mathbf{u}_o = (-ys, xs)^T$ with $s = (x^2 + y^2 - 4)e^{-(x^2+y^2)(x^2+y^2-8)/8}/32$.

coarse-grained particle density $\rho_p(K, t)$ agrees closely with the continuum density $\rho(\mathbf{x}, t)$, with small deviations attributable to finite sampling, discrete advection errors, and local rearrangements induced by collisions. We remark that the coarse-grained particle mass density $\rho_p(K, t)$ appears non-smooth because it is obtained by binning a finite number of discrete flocs into grid cells, so finite-sampling (shot-noise) fluctuations and occasional collision-induced clustering produce cell-to-cell jumps. Theoretically, it would become smoother, as the number of particles goes to infinity. We observe similar non-smoothness in velocities and angular velocities.

- *Velocity consistency and alignment with the ocean flow.* Starting from $\mathbf{v}^i(0) = \mathbf{0}$ and $\mathbf{u}(\mathbf{x}, 0) = \mathbf{0}$, both models accelerate toward the prescribed ocean velocity field $\mathbf{u}_o(\mathbf{x})$ through the same quadratic drag mechanism:

$$\alpha^i(\mathbf{u}_o^i - \mathbf{v}^i)|\mathbf{u}_o^i - \mathbf{v}^i| \quad \text{in (2.1c),} \quad \bar{\alpha}(\mathbf{u}_o - \mathbf{u})|\mathbf{u}_o - \mathbf{u}| \quad \text{in (4.15b).}$$

The spatial patterns of $\mathbf{u}_p(K, t)$ and $\mathbf{u}(\mathbf{x}, t)$ agree well, and the difference field remains small throughout the simulation. In particular, by $T = 10$ the computed velocities in both models are close to $\mathbf{u}_o(\mathbf{x})$, indicating that the particle ensemble and the continuum drift converge toward the same ocean-driven equilibrium,

though we do not have a theorem for the velocity alignment when the ocean velocity varies in space.

- *Angular velocity consistency.* The angular velocity moments also exhibit strong agreement. The particle angular velocities $\omega^i(t)$ are driven toward $\frac{1}{2}\nabla \times \mathbf{u}_o(\mathbf{x}^i(t))$ through the rotational drag in (2.1d), while the continuum moment $\bar{\omega}(\mathbf{x}, t)$ is driven by the corresponding term in (4.15c). The coarse-grained particle moment $\bar{\omega}_p(K, t)$ reproduces the continuum field $\bar{\omega}(\mathbf{x}, t)$ well, capturing both the sign structure and the magnitude distribution induced by the nonuniform vorticity of \mathbf{u}_o .
- *Overall consistency of the hierarchy.* Taken together, the agreement of $(\rho, \mathbf{u}, \bar{\omega})$ between the continuum solver and the coarse-grained particle statistics at multiple times supports the consistency of the particle-to-continuum closure in the monokinetic regime, and provides numerical validation for the particle–kinetic–hydrodynamic hierarchy developed in this work. Moreover, one expects better agreement as the number of particles increases and as the time-step and mesh grid sizes are finer for higher numerical accuracy.

In summary, Examples 1–2 provide complementary validation of the particle dynamics and the particle–kinetic–hydrodynamic hierarchy developed in this work. In Example 1, we simulate $n = 100$ rotating, colliding floes in the periodic domain $\Omega = [-\pi, \pi]^2$ under a constant ocean velocity $\mathbf{u}_o \equiv (0.3, 0)^T$. The results confirm the theoretical long-time velocities and angular velocity alignment with the ocean velocity. The corresponding kinetic energies exhibit the expected dissipative trends, while momentum and angular momentum satisfy the correct balance laws in the presence of ocean drag. In Example 2, we retain the same domain, time stepping, and physical parameters, but impose a spatially varying rotational ocean flow and place $n = 10^4$ identical floes on a 100×100 lattice with zero initial velocities. Solving the continuum system (4.15) on a 50×50 grid using a linear finite element mesh and coarse-graining the particle data onto the same grid, we find that the particle and continuum fields match well, demonstrating that the hydrodynamic closure reproduces the coarse-scale statistics of the particle model and thereby supporting the consistency of the proposed multiscale hierarchy.

6 Concluding remarks

In this paper, we have extended the particle–kinetic–hydrodynamic hierarchy developed in Part I to a substantially richer and more realistic setting by incorporating rotational degrees of freedom and nonlinear contact interactions among sea-ice floes. Starting from a rigid-body particle description with force–torque coupling, we derived an associated kinetic equation on an extended phase space and obtained macroscopic hydrodynamic balance laws for mass, linear momentum, and angular momentum through moment closures. We established the total energy dissipation, which captures the physics of energy loss due to the floe–floe collision. The resulting framework reveals how nonlinear collisions, frictional effects, and rotational dynamics generate additional stress and dissipa-

tion mechanisms at the macroscopic level, thereby providing a systematic and physically consistent multiscale description of fragmented sea ice in the marginal ice zone.

Several important directions remain open for future research. One natural extension is to couple the present mechanical framework with a temperature field, allowing floe sizes, masses, and moments of inertia to evolve through melting and refreezing processes. Such a thermo-mechanical coupling would introduce additional transport and source terms at all scales and raise fundamental questions about energy consistency, scale separation, and closure strategies, leading to more realistic sea ice rheology. Another challenging direction concerns floe fracture and bonding, corresponding to a dynamically varying number of particles due to breakup, aggregation, or refreezing-induced bonding. From a modeling and analytical perspective, this leads to nontrivial difficulties in tracking collective behavior, conservation laws, and statistical descriptions, when the underlying particle number changes in time. Developing a coherent multiscale theory that accommodates variable particle numbers while retaining tractable kinetic and hydrodynamic limits remains an open and promising problem for future study.

Acknowledgements

Q.D. is partially supported by the start-up funding from the Yau Mathematical Sciences Center, Tsinghua University, the Australian National Computing Infrastructure (NCI) national facility under grant zv32, and the work of S.-Y. Ha is supported by National Research Foundation(NRF) grant funded by the Korea government(MIST) (RS-2025-00514472).

References

- [1] A. ALBERELLO, L. BENNETTS, P. HEIL, C. EAYRS, M. VICHI, K. MACHUTCHON, M. ONORATO, AND A. TOFFOLI, *Drift of pancake ice floes in the winter antarctic marginal ice zone during polar cyclones*, Journal of Geophysical Research: Oceans, 125 (2020), p. e2019JC015418.
- [2] A. ALBERELLO, L. G. BENNETTS, M. ONORATO, M. VICHI, K. MACHUTCHON, C. EAYRS, B. N. NTAMBA, A. BENETAZZO, F. BERGAMASCO, F. NELLI, ET AL., *Three-dimensional imaging of waves and floes in the marginal ice zone during a cyclone*, Nature Communications, 13 (2022), p. 4590.
- [3] C. BARDOS, F. GOLSE, AND D. LEVERMORE, *Fluid dynamic limits of kinetic equations. I. Formal derivations*, Journal of statistical physics, 63 (1991), pp. 323–344.
- [4] A. BATESON, D. FELTHAM, D. SCHRÖDER, S. DURSKI, J. HUTCHINGS, R. BASU, AND B. HWANG, *Simulating in-plane failure of sea ice floes in the arctic using discrete element methods*, in EGU General Assembly Conference Abstracts, 2025, pp. EGU25–5195.

- [5] L. BENNETTS, C. BITZ, D. FELTHAM, A. KOHOUT, AND M. MEYLAN, *Marginal ice zone dynamics: future research perspectives and pathways*, Philosophical Transactions of the Royal Society A, 380 (2022), p. 20210267.
- [6] L. G. BENNETTS, C. M. BITZ, D. L. FELTHAM, A. L. KOHOUT, AND M. H. MEYLAN, *Theory, modelling and observations of marginal ice zone dynamics: multidisciplinary perspectives and outlooks*, 2022.
- [7] E. BLOCKLEY, M. VANCOPPENOLLE, E. HUNKE, C. BITZ, D. FELTHAM, J.-F. LEMIEUX, M. LOSCH, E. MAISONNAVE, D. NOTZ, P. RAMPAL, ET AL., *The future of sea ice modeling: where do we go from here?*, Bulletin of the American Meteorological Society, 101 (2020), pp. E1304–E1311.
- [8] N. N. BOGOLIUBOV, *Kinetic equations*, Zhurnal Eksperimental'noi i Teoreticheskoi Fiziki, 16 (1946), pp. 691–702.
- [9] N. N. BOGOLIUBOV, *Kinetic equations*, Journal of Physics USSR, 10 (1946), pp. 265–274.
- [10] M. BORN AND H. S. GREEN, *A general kinetic theory of liquids I. the molecular distribution functions*, Proceedings of the Royal Society of London. Series A. Mathematical and Physical Sciences, 188 (1946), pp. 10–18.
- [11] R. H. BOURKE AND R. P. GARRETT, *Sea ice thickness distribution in the Arctic ocean*, Cold Regions Science and Technology, 13 (1987), pp. 259–280.
- [12] J. C. BUTCHER, *Numerical methods for ordinary differential equations*, John Wiley & Sons, 2016.
- [13] C. CERCIGNANI, R. ILLNER, AND M. PULVIRENTI, *The mathematical theory of dilute gases*, vol. 106, Springer Science & Business Media, 2013.
- [14] N. CHEN, Q. DENG, AND S. STECHMANN, *Superfloe parameterization with physics constraints for uncertainty quantification of sea ice floes*, SIAM/ASA Journal on Uncertainty Quantification, 10 (2022), pp. 1384–1409.
- [15] N. CHEN, S. FU, AND G. E. MANUCHARYAN, *An efficient and statistically accurate Lagrangian data assimilation algorithm with applications to discrete element sea ice models*, Journal of Computational Physics, 455 (2022), p. 111000.
- [16] M. D. COON, G. A. MAYKUT, R. S. PRITCHARD, D. A. ROTHROCK, AND A. S. THORNDIKE, *Modeling the pack ice as an elastic-plastic material*, AIDJEX Bull., No. 24 (1974), p. 105pp.
- [17] P. A. CUNDALL AND O. D. STRACK, *A discrete numerical model for granular assemblies*, Geotechnique, 29 (1979), pp. 47–65.

- [18] A. DAMSGAARD, A. ADCROFT, AND O. SERGIENKO, *Application of discrete element methods to approximate sea ice dynamics*, Journal of Advances in Modeling Earth Systems, 10 (2018), pp. 2228–2244.
- [19] V. DANSEREAU, J. WEISS, P. SARAMITO, AND P. LATTES, *A Maxwell elasto-brittle rheology for sea ice modelling*, The Cryosphere, 10 (2016), pp. 1339–1359.
- [20] G. G. DE DIEGO, M. GUPTA, S. A. GERING, R. HARIS, AND G. STADLER, *Modelling sea ice in the marginal ice zone as a dense granular flow with rheology inferred from discrete element model data*, Journal of Fluid Mechanics, 1000 (2024), p. A22.
- [21] Q. DENG, N. CHEN, S. N. STECHMANN, AND J. HU, *Lemda: A lagrangian-eulerian multiscale data assimilation framework*, Journal of Advances in Modeling Earth Systems, 17 (2025), p. e2024MS004259.
- [22] Q. DENG AND A. ERN, *Softfem: revisiting the spectral finite element approximation of second-order elliptic operators*, Computers & Mathematics with Applications, 101 (2021), pp. 119–133.
- [23] Q. DENG AND S.-Y. HA, *Particle, kinetic and hydrodynamic models for sea ice floes. part i: Non-rotating floes*, Physica D: Nonlinear Phenomena, 483 (2025), p. 134951.
- [24] Q. DENG, S. N. STECHMANN, AND N. CHEN, *Particle-continuum multiscale modeling of sea ice floes*, Multiscale Modeling & Simulation, 22 (2024), pp. 230–255.
- [25] J. W. DUFTY, *Kinetic theory and hydrodynamics for a low density granular gas*, Advances in Complex Systems, 4 (2001), pp. 397–406.
- [26] L. C. EVANS, *Partial differential equations*, vol. 19, American mathematical society, 2022.
- [27] D. L. FELTHAM, *Sea ice rheology*, Annu. Rev. Fluid Mech., 40 (2008), pp. 91–112.
- [28] A. FIGALLI AND M.-J. KANG, *A rigorous derivation from the kinetic Cucker–Smale model to the pressureless euler system with nonlocal alignment*, Analysis & PDE, 12 (2018), pp. 843–866.
- [29] K. M. GOLDEN, L. G. BENNETTS, E. CHERKAEV, AND ET AL., *Modeling sea ice*, Notices Amer. Math. Soc., 67 (2020), pp. 1535–1555.
- [30] F. GOLSE, *The mean-field limit for the dynamics of large particle systems*, Journées équations aux dérivées partielles, (2003), pp. 1–47.
- [31] ———, *The Boltzmann equation and its hydrodynamic limits*, in Handbook of Differential Equations: Evolutionary Equations, vol. 2, Elsevier, 2005, pp. 159–301.

- [32] ———, *On the dynamics of large particle systems in the mean field limit*, in *Macroscopic and large scale phenomena: coarse graining, mean field limits and ergodicity*, Springer, 2016, pp. 1–144.
- [33] T. H. GRONWALL, *Note on the derivatives with respect to a parameter of the solutions of a system of differential equations*, *Annals of Mathematics*, 20 (1919), pp. 292–296.
- [34] Z. M. GUDKOVICH AND Y. G. NIKIFOROV, *Stationary drift of a single floe*, *Tr. Arkt. Anarkt.*, 253 (1963).
- [35] D. GUGAN, *Inelastic collision and the hertz theory of impact*, *American Journal of Physics*, 68 (2000), pp. 920–924.
- [36] S.-Y. HA AND E. TADMOR, *From particle to kinetic and hydrodynamic descriptions of flocking*, *Kinetic and Related Models*, 1 (2008), pp. 415–435.
- [37] E. HAIRER, S. P. NØRSETT, AND G. WANNER, *Solving ordinary differential equations. 1, Nonstiff problems*, Springer-Verlag, 1993.
- [38] A. HERMAN, *Discrete-element bonded-particle sea ice model design, version 1.3 a-model description and implementation*, *Geoscientific Model Development*, 9 (2016), pp. 1219–1241.
- [39] ———, *Granular effects in sea ice rheology in the marginal ice zone*, *Philosophical Transactions of the Royal Society A*, 380 (2022), p. 20210260.
- [40] A. HERMAN, S. CHENG, AND H. H. SHEN, *Wave energy attenuation in fields of colliding ice floes—part 1: Discrete-element modelling of dissipation due to ice–water drag*, *The Cryosphere*, 13 (2019), pp. 2887–2900.
- [41] H. HERTZ, *Ueber die berührung fester elastischer körper.*, *Journal für die reine und angewandte Mathematik*, 1882 (1882), pp. 156–171.
- [42] W. HIBLER III, *A dynamic thermodynamic sea ice model*, *Journal of physical oceanography*, 9 (1979), pp. 815–846.
- [43] M. A. HOPKINS, *A discrete element Lagrangian sea ice model*, *Engineering Computations*, (2004).
- [44] T. J. HUGHES, *The finite element method: linear static and dynamic finite element analysis*, Courier Corporation, 2003.
- [45] E. HUNKE AND J. DUKOWICZ, *An elastic–viscous–plastic model for sea ice dynamics*, *Journal of Physical Oceanography*, 27 (1997), pp. 1849–1867.
- [46] E. HUNKE, D. NOTZ, A. TURNER, AND M. VANCOPPENOLLE, *The multiphase physics of sea ice: a review for model developers*, *The Cryosphere*, 5 (2011), pp. 989–1009.

- [47] E. C. HUNKE, W. H. LIPSCOMB, AND A. K. TURNER, *Sea-ice models for climate study: retrospective and new directions*, Journal of Glaciology, 56 (2010), pp. 1162–1172.
- [48] K. L. JOHNSON, *Contact mechanics*, Cambridge university press, 1987.
- [49] G. KARNIADAKIS, A. BESKOK, AND N. ALURU, *Microflows and nanoflows: fundamentals and simulation*, Springer, 2005.
- [50] J. G. KIRKWOOD, *The statistical mechanical theory of transport processes I. general theory*, The Journal of Chemical Physics, 14 (1946), pp. 180–201.
- [51] H. LI, E. D. GEDIKLI, R. LUBBAD, AND T. S. NORD, *Laboratory study of wave-induced ice-ice collisions using robust principal component analysis and sensor fusion*, Cold Regions Science and Technology, 172 (2020), p. 103010.
- [52] R. LINDSAY AND H. STERN, *A new Lagrangian model of Arctic sea ice*, Journal of physical oceanography, 34 (2004), pp. 272–283.
- [53] S. LUDING, *Introduction to discrete element methods: basic of contact force models and how to perform the micro-macro transition to continuum theory*, European journal of environmental and civil engineering, 12 (2008), pp. 785–826.
- [54] G. E. MANUCHARYAN AND B. P. MONTEMURO, *SubZero: A sea ice model with an explicit representation of the floe life cycle*, Journal of Advances in Modeling Earth Systems, (2022), p. e2022MS003247.
- [55] M. H. MEYLAN, C. HORVAT, C. M. BITZ, AND L. G. BENNETTS, *A floe size dependent scattering model in two-and three-dimensions for wave attenuation by ice floes*, Ocean Modelling, 161 (2021), p. 101779.
- [56] F. NANSEN, *The Norwegian North Polar Expedition, 1893-1896: Scientific Results*, vol. 3, Longmans, Green and Company, 1902.
- [57] J. F. NYE, *The motion of ice sheets and glaciers*, Journal of Glaciology, 3 (1959), pp. 493–507.
- [58] C. L. PARKINSON AND W. M. WASHINGTON, *A large-scale numerical model of sea ice*, Journal of Geophysical Research: Oceans, 84 (1979), pp. 311–337.
- [59] T. PÖSCHEL AND T. SCHWAGER, *Computational granular dynamics: models and algorithms*, Springer Science & Business Media, 2005.
- [60] M. PUTTOCK, E. THWAITE, ET AL., *Elastic compression of spheres and cylinders at point and line contact*, Commonwealth Scientific and Industrial Research Organization Melbourne, 1969.

- [61] L. A. ROACH, C. HORVAT, S. M. DEAN, AND C. M. BITZ, *An emergent sea ice floe size distribution in a global coupled ocean-sea ice model*, Journal of Geophysical Research: Oceans, 123 (2018), pp. 4322–4337.
- [62] L. SAINT-RAYMOND, *Hydrodynamic limits of the Boltzmann equation*, Springer, 2009.
- [63] H. H. SHEN, W. D. HIBLER III, AND M. LEPPÄRANTA, *The role of floe collisions in sea ice rheology*, Journal of Geophysical Research: Oceans, 92 (1987), pp. 7085–7096.
- [64] H. L. STERN, A. J. SCHWEIGER, M. STARK, J. ZHANG, M. STEELE, B. HWANG, AND T. MAKSYM, *Seasonal evolution of the sea-ice floe size distribution in the Beaufort and Chukchi seas*, Elementa: Science of the Anthropocene, 6 (2018).
- [65] A. S. THORNDIKE, D. ROTHROCK, G. MAYKUT, AND R. COLONY, *The thickness distribution of sea ice*, Journal of Geophysical Research, 80 (1975), pp. 4501–4513.
- [66] S. TOPPALADODDI AND J. S. WETTTLAUER, *Theory of the sea ice thickness distribution*, Physical review letters, 115 (2015), p. 148501.
- [67] T. TOYOTA, C. HAAS, AND T. TAMURA, *Size distribution and shape properties of relatively small sea-ice floes in the antarctic marginal ice zone in late winter*, Deep Sea Research Part II: Topical Studies in Oceanography, 58 (2011), pp. 1182–1193.
- [68] J. WEISS AND V. DANSEREAU, *Linking scales in sea ice mechanics*, Philosophical Transactions of the Royal Society A: Mathematical, Physical and Engineering Sciences, 375 (2017), p. 20150352.
- [69] A. V. WILCHINSKY AND D. L. FELTHAM, *Modelling the rheology of sea ice as a collection of diamond-shaped floes*, Journal of non-newtonian fluid mechanics, 138 (2006), pp. 22–32.
- [70] J. YVON AND Y. ROCARD, *La théorie statistique des fluides et l'équation d'état*, Actual. Sci. & Indust., (1935).

Appendix A: Local Homogeneity Assumption

In the derivation of macroscopic balance laws (4.15) from the kinetic description of sea ice, we adopted the local homogeneity assumption to further simplify the integrals on contact operator in (4.10) and (4.11). This assumption formalizes the notion that, at sufficiently small scales around a given macroscopic position, the ice floe distribution exhibits negligible spatial gradients. Under this somewhat strong assumption, contact-operator related terms vanish in analogy with [3, 30, 31] for gas particles, enabling the simplified hydrodynamic equations (4.15).

(Local homogeneity assumption) We say that $F(\mathbf{x}, \mathbf{v}, \theta, \omega, r, h)$ is locally homogeneous at \mathbf{x} if, for \mathbf{s} in a neighborhood of zero with $|\mathbf{s}| \ll L$ for some macroscopic scale $L > 0$,

$$F(t, \mathbf{x} + \mathbf{s}, \mathbf{v}, \theta, \omega, r, h) \approx F(t, \mathbf{x}, \mathbf{v}, \theta, \omega, r, h),$$

and similarly for its moments. This condition asserts that the distribution varies slowly relative to the characteristic length scales of the collision/contact interactions.

The local homogeneity assumption reflects the physical idea that, at scales comparable with the interaction range of flocs (e.g., contact kernel support), the macroscopic fields vary negligibly. In other words, the spacing between colliding or interacting flocs is small relative to macroscopic gradients in density and velocity. This justifies treating F and its moments as essentially constant over the support of the collision/contact operator.

Recall (4.14) that

$$\begin{aligned} \mathcal{T}_{52} &= \int_{\hat{\mathbb{R}}_3} m \mathbf{f}_{c,n}[F](t, \mathbf{z}) F(t, \mathbf{y}) d\mathbf{y} \\ &= \int_{\hat{\mathbb{R}}_3} \int_{\hat{\mathbb{R}}_4} m \kappa_1(|\mathbf{x}^* - \mathbf{x}| - (r + r^*)) \mathbf{n}(\mathbf{x}, \mathbf{x}^*) F(t, \mathbf{z}^*) d\mathbf{z}^* F(t, \mathbf{y}) d\mathbf{y}, \end{aligned}$$

where $\mathbf{y} = (\mathbf{v}, \theta, \omega, r, h)$, $\mathbf{z}^* = (\mathbf{x}^*, \mathbf{v}^*, \theta^*, \omega^*, r^*, h^*)$. Using the local homogeneity assumption and exchange of variables, the internal integration is approximated as

$$\begin{aligned} m \mathbf{f}_{c,n}[F](t, \mathbf{z}) &= \int_{\hat{\mathbb{R}}_4} m \kappa_1(|\mathbf{x}^* - \mathbf{x}| - (r + r^*)) \mathbf{n}(\mathbf{x}, \mathbf{x}^*) F(t, \mathbf{x}^*, \mathbf{y}^*) d\mathbf{x}^* d\mathbf{y}^* \\ &= \int_{\hat{\mathbb{R}}_4} m \kappa_1(|\mathbf{x} - \mathbf{x}^*| - (r^* + r)) \mathbf{n}(\mathbf{x}^*, \mathbf{x}) F(t, \mathbf{x}, \mathbf{y}^*) d\mathbf{x} d\mathbf{y}^* \\ &= - \int_{\hat{\mathbb{R}}_4} m \kappa_1(|\mathbf{x}^* - \mathbf{x}| - (r + r^*)) \mathbf{n}(\mathbf{x}, \mathbf{x}^*) F(t, \mathbf{x}, \mathbf{y}^*) d\mathbf{x} d\mathbf{y}^* \\ &= \frac{1}{2} \int_{\hat{\mathbb{R}}_4} m \kappa_1(|\mathbf{x}^* - \mathbf{x}| - (r + r^*)) \mathbf{n}(\mathbf{x}, \mathbf{x}^*) (F(t, \mathbf{x}^*, \mathbf{y}^*) d\mathbf{x}^* - F(t, \mathbf{x}, \mathbf{y}^*) d\mathbf{x}) d\mathbf{y}^* \\ &\approx 0, \end{aligned}$$

where the last approximation is based on the local homogeneity assumption of moments. Thus, $\mathcal{T}_{52} \approx 0$. This may be interpreted as the collisional force being approximately zero (forces surrounding a floe at \mathbf{x} cancel) in the distribution sense, as the number of flocs goes to infinity, assumed in Section 3 for kinetic description. Similarly, one can derive $\mathcal{T}_{53} \approx 0$ and using this local assumption and that $(\mathbf{v} - \mathbf{v}^*) \cdot \mathbf{n}(\mathbf{x}, \mathbf{x}^*) = (\mathbf{v}^* - \mathbf{v}) \cdot \mathbf{n}(\mathbf{x}^*, \mathbf{x})$ and $\mathcal{T}_{54} \approx 0$ using $\mathbf{t}(\mathbf{x}, \mathbf{x}^*) = -\mathbf{t}(\mathbf{x}^*, \mathbf{x})$. The term $\mathbf{x} \times \mathcal{T}_{54} + \mathcal{T}_{56}$ vanishes following a similar derivation in (2.13). This leads to the simplified hydrodynamic model (4.15) which was studied in the numerical experiments in Section 5.

On the other hand, the local homogeneity assumption have limitations. It is a heuristic approximation that ensures the contact operator conserves mass and momentum as in [3, 30, 31] for gas particles. However, sea ice floe particles, with different Knudsen number [49], are different from gas particles (typically for dilute regime with small

rare collisions, i.e., Boltzmann–Grad limit). They are most justified when macroscopic gradients vary on scales much larger than the contact interaction range. In regimes with strong shear or boundary effects, deviations from local homogeneity should be considered and this would lead to more realistic sea ice rheology [27, 39, 63].

We take the momentum balance law (4.9b) as an example to derive the contact stress tensor as in sea ice rheology discussed in [27]. We recall the balance law for momentum in (4.9b):

$$\partial_t(\rho\mathbf{u}) + \nabla_{\mathbf{x}} \cdot (\rho\mathbf{u} \otimes \mathbf{u}) = \int_{\hat{\mathbb{R}}_3} m\mathbf{f}[F]F d\mathbf{y}, \quad \mathbf{f}[F] = \mathbf{f}_o + \mathbf{f}_c[F],$$

where $\mathbf{f}_o = \gamma_o(\mathbf{u}_o - \mathbf{v})|\mathbf{u}_o - \mathbf{v}|$ and $\mathbf{f}_c[F](t, \mathbf{z}) = \int_{\hat{\mathbb{R}}_4} \mathbf{f}_c(\mathbf{z}, \mathbf{z}^*)F(t, \mathbf{z}^*)d\mathbf{z}^*$ with $\mathbf{f}_c(\mathbf{z}, \mathbf{z}^*)$ containing the normal, damping, and tangential components defined in (3.12). With mono-kinetic ansatz (4.7), we define and calculate the contact contribution

$$\begin{aligned} \mathbf{b}_c(t, \mathbf{x}) &:= \int_{\hat{\mathbb{R}}_3} m\mathbf{f}_c[F](t, \mathbf{x}, \mathbf{y})F(t, \mathbf{x}, \mathbf{y})d\mathbf{y} \\ &= \int_{\hat{\mathbb{R}}_3} \int_{\hat{\mathbb{R}}_4} m(\mathbf{y})\mathbf{f}_c(\mathbf{z}, \mathbf{z}^*)F(t, \mathbf{z})F(t, \mathbf{z}^*)d\mathbf{z}^*d\mathbf{y} \\ &= \rho(t, \mathbf{x}) \int_{\hat{\mathbb{R}}_3} \int_{\hat{\mathbb{R}}_4} \Phi \frac{\rho(t, \mathbf{x}^*)}{m(r^*, h^*)} \Phi^* \mathbf{f}_c(\mathbf{z}, \mathbf{z}^*)d\mathbf{z}^*d\mathbf{y}, \end{aligned}$$

where $\Phi = \Phi(t, \mathbf{x}, \theta, r, h)$ and $\Phi^* = \Phi(t, \mathbf{x}^*, \theta^*, r^*, h^*)$. To obtain the contact stress tensor, we adopt the Irving–Kirkwood form and introduce the bond-localization kernel

$$B(\mathbf{x}; \mathbf{x}, \mathbf{x}^*) := \int_0^1 \hat{\delta}(\mathbf{x} - (1-s)\mathbf{x} - s\mathbf{x}^*)ds,$$

and use the standard Irving–Kirkwood identity

$$\nabla_{\mathbf{x}} \cdot ((\mathbf{x}^* - \mathbf{x})B(\mathbf{x}; \mathbf{x}, \mathbf{x}^*)) = \hat{\delta}(\mathbf{x} - \mathbf{x}^*) - \hat{\delta}(\mathbf{x} - \mathbf{x}).$$

Then the contact force density admits the stress representation

$$\mathbf{b}_c(t, \mathbf{x}) = \nabla_{\mathbf{x}} \cdot \sigma_c^{\text{MK}}(t, \mathbf{x}),$$

where the monokinetic contact stress tensor is

$$\sigma_c^{\text{MK}}(t, \mathbf{x}) = -\frac{1}{2} \int_{\hat{\mathbb{R}}_4^2} (\mathbf{x}^* - \mathbf{x}) \otimes (\rho(t, \mathbf{x})\Phi) \frac{\rho(t, \mathbf{x}^*)}{m(r^*, h^*)} \Phi^* \mathbf{f}_c(\mathbf{z}, \mathbf{z}^*)B(\mathbf{x}; \mathbf{x}, \mathbf{x}^*)d\mathbf{z}^*d\mathbf{y}$$

Moreover, one may decompose the terms as $\sigma_c^{\text{MK}} = \sigma_{\mathbf{n}}^{\text{MK}} + \sigma_{\mathbf{v}}^{\text{MK}} + \sigma_{\mathbf{t}}^{\text{MK}}$, obtained by replacing \mathbf{f}_c by \mathbf{f}_n , \mathbf{f}_v , and \mathbf{f}_t , respectively. Using the contact stress tensor, the momentum balance law (4.9b) reduces to

$$\partial_t(\rho\mathbf{u}) + \nabla_{\mathbf{x}} \cdot (\rho\mathbf{u} \otimes \mathbf{u}) = \nabla_{\mathbf{x}} \cdot \sigma_c^{\text{MK}} + \bar{\alpha}(\mathbf{u}_o - \mathbf{u})|\mathbf{u}_o - \mathbf{u}|,$$

where $\bar{\alpha}$ is defined in (4.12). Herein, the right-hand side consists of a contact stress divergence and an effective ocean drag as in sea ice rheology discussed in [27, 39, 42, 63]. We remark that the balance law for angular momentum can be developed similarly. Incorporating rotational effects enriches the continuum description of sea ice rheology in the literature; a detailed development will be pursued in future work.